Changes in flow and sediment trapping caused by bioturbating macrofauna (*austrohelice crassa*)

A thesis

submitted in partial fulfilment

of the requirements for the degree

of

MSc (Research)

at

The University of Waikato

by

HOLLY KATE JOSEPHINE BREDIN-GREY

THE UNIVERSITY OF
WAIKATO
Te Whare Wānanga o Waikato

2016

ABSTRACT

Intertidal ecosystems contribute a significant portion of the world's ecosystem goods and services. Recently, an increasing amount of focus has been generated surrounding the central role of sediment mixing (bioturbation) in estuarine ecosystems. Bioturbating macrofauna such as the burrowing mud crab *austrohelice crassa* are found in many New Zealand ecosystems, and have been shown to be key ecosystem engineers in these environments. Burrow building extends the sediment-water interface, creating changes in solute and particle fluxes through modification of near-bed flows. Burrows and holes have been poorly studied compared with their above-ground counterparts and the exact manner in which burrows affect small-scale water movement at the sediment water interface is yet to be understood.

This project used measurements of fine scale flows surrounding *austrohelice crassa* burrows *in situ* as well as in a laboratory setting. Experiments used artificial burrows in a unidirectional flume to explore the impact that crab burrow orientation has on flow. Measurements of flow velocities were taken and it was found that flow extended further into the burrow when the burrow was aligned downstream with the flow rather than at right angles or aligned upstream to the flow.

Subsequently, the impact of burrow density on near-bed flows was quantified in the laboratory using different density arrays of artificial burrows. Measurements of velocity were used to calculate turbulent kinetic energy (TKE). It was found that with increasing burrow density there was a split in flow regimes

between high and low flow speeds. At low flow speeds, the TKE increased to a peak followed by a decline, owing to the development of skimming flow.

Field experiments examined flows around arrays of artificial and natural burrows including a control, a sparse, and a dense artificial burrow array (0, 40, and 74 burrows/m^2, respectively), as well as a control, a sparse, and a dense array of natural burrows (0, 30, and 62 burrows/m^2, respectively). Measurements taken within these arrays found that for the artificial burrow array, TKE appeared to increase to a peak for the sparse array, and decreased again for the dense array. This relationship is similar to that found in the burrow array laboratory experiment. For the natural burrow array, TKE increased with burrow density. For all field experiments combined, a split in flow regimes between high and low flow speeds emerges, similar to the split found in the laboratory experiments.

Sediment trapping within the artificial burrows was measured for over one tidal cycle. It was found that the dense array trapped a greater amount of sediment (1.95 g/L) compared with the sparse array (1.66 g/L). Overall, it appeared that the sediment caught within the burrows had a greater proportion of silt when compared with the local surficial sediment, indicating the possibility of ecosystem engineering. Volumes trapped of this magnitude have considerable potential to alter the morphology of tidal flats. Overall, these results offer intriguing insight into the role of burrowing fauna in affecting flows and sediment fluxes on intertidal sandflats.

ACKNOWLEDGEMENTS

I would like to thank the many people who have helped me in one way or another to complete my masters.

First and foremost I would like to acknowledge my chief supervisor, Julia Mullarney (University of Waikato), as her encouragement, knowledge, and guidance proved invaluable in creating this thesis. Julia's dedication, creativity, and enthusiasm was infectious; providing much-needed boosts throughout the past two years. I would also like to thank my secondary supervisors, Drew Lohrer (NIWA), and Conrad Pilditch (University of Waikato). I greatly appreciate all the time and effort that Conrad, Julia, and Drew spent on inspiring and steering the direction of my research as well as providing essential advice along the way.

A special thank you to Hazel Needham (University of Waikato) who has given vital insight and knowledge into the biology of *austrohelice crassa*, as well as lending an essential hand with chilly winter field work. I would also like to acknowledge Dean Sandwell for his invaluable help in the laboratory building crab burrow replicas. I must also thank the Earth Sciences Department, my peers, and administrative staff for guiding me through the past two years.

To my parents and friends, thank you for providing much needed time out, motivation and for being with me every step of the way. Without your support I would have not made it to this stage in my life.

I would also like to thank the various institutions which provided me with funding for my masters including: The University of Waikato Masters Research

Scholarship, the University of Waikato External Research Provider Development Grant, the Waikato Graduate Women Educational Trust, the Broad Memorial Fund, and the Terry Healy Memorial Award. Without this funding, this research would not have been possible.

TABLE OF CONTENTS

LIST OF FIGURES

LIST OF TABLES

CHAPTER ONE: INTRODUCTION

1.1 Motivation

New Zealand soft sediment ecosystems provide numerous ecosystem goods and services such as carbon sequestration, nutrient cycling, and primary production (Snelgrove, 1999; Webb & Eyre, 2004c). Shallow estuarine sediments are influenced by terrestrial, freshwater, and marine environments and are sites of intricate biophysical and geochemical interactions (Pritchard, 1967). The way estuarine ecosystems function is defined by complex processes. These functions can have dynamic responses to environmental changes such as those caused by biota within the bed sediment. Benthic soft-sediment fauna alter their habitat as they move and feed, reworking sediment and creating three-dimensional topographic relief. In recent years an increasing amount of focus has been generated surrounding the central role of bioturbation (the mixing and reworking of sediment by organisms) in estuarine ecosystems, although there still remain significant questions on the effect that burrows/holes have on flows and sediment trapping.

1.1.1 Burrows in the Environment

Bioturbating crabs occupy much of the intertidal environment, and many create burrows for protection from predators. These burrows can be of varying densities, and sizes. The bioturbating macrofauna *austrohelice crassa* (herein referred to as *austrohelice crassa* or the mud crab) were first described by Dana (1851), and reside in large numbers in the upper intertidal areas of soft sediment systems around New Zealand (Gibbs et al., 2001; Needham, 2011a). Mud crab typically share an estuarine habitat with one other crab species (*macrophthalmus hirtipes*) (Hawkins

& Jones, 1982). *Austrohelice crassa* usually occupy muddy mid-high intertidal sediments, whereas *macrophthalmus hirtipes* are found on mid-lower intertidal areas (Nye, 1977). A significant aspect of *austrohelice crassa* behaviour which influences the surrounding environment is the building and maintenance of burrows. Although little is known about the social behaviour of *austrohelice crassa*; it has been suggested that the mud crab build burrows for predatory defence reasons. *Austrohelice crassa* are deposit feeders which leave surficial pellets on the sediment bed while feeding changing the bed topography, and excrete ammonia (Needham, 2011b). Their burrows are created through the process of rolling pellets from the sub-bottom sediment out onto the surface. These pellets are visibly darker than those produced from deposit feeding. The fauna's mode of feeding can also cause an increase in topographic roughness attributed to the deposition of surficial pellets (Hollins et al., 2009; Needham et al., 2013).

Burrow building and pellet deposition impacts the sediment-water interface, and alters flow close to the sea bed, creating changes in the nature of chemical, physical, and biological interactions in these regions. Thus, these mud crabs are known ecosystem engineers and have been identified as key species in their natural environments (Warren & Underwood, 1986; Thrush et al., 2003; Needham, 2011b).

The burrows of *austrohelice crassa* have been shown to exhibit a variety of shapes and sizes (Morrisey et al., 1999; Needham et al., 2010). The structure of the burrows is often that of tunnels and galleries (Morrisey et al., 1999). Burrow morphology may take the form of a cone, u-, j-, i-, y-, inverted y-, branching, or complex shape (Figure 1). It has been shown that sediment type may be a major control on the dominant burrow shape and burrow density (Needham et al., 2013).

Generally, in sandier sediment burrows take the dominant form of a j-, i-, or inverted y- shape, and arrays are less dense. In muddier areas the dominant burrow form is a i-, or j- shape, and assemblages are more dense (Needham et al., 2010). The burrows have been found to extend as far as 0.28 m into the sediment (Morrisey et al., 1999). Needham et al. (2010) found that the median burrow depth was 47 and 39 mm for mud and sand environments, respectively. *Austrohelice crassa* burrows do not appear to have a preferred orientation to flow direction (H. Needham, personal communication, 9 July, 2015). The orientation of prawn burrows has also been shown to be random in the field, showing no alignment to current direction (Allanson et al., 1992). The extent of burrow area has been shown to be dependent on environmental conditions (Kristensen & Kosta, 2005). As a result, crabs of the same species may build burrows of distinctly different structures. Indeed, *austrohelice crassa* have been found to exhibit different burrow building behaviour in different sediment types (Needham et al., 2013). Burrow building can involve the excavation of long connected tunnels, resulting in a mound being deposited at the burrow entrance, changing the surface topography. Such a change in topography will result in an alteration of flow velocities, advective pore water flows, and bed shear stress, as well as an increase in bed roughness (Ziebis et al., 1996; Botto & Iribarne, 2000; Widdows & Brinsley, 2002).

Figure 1: Burrow shapes of austrohelice crassa found by Needham et al. (2011). Left to right: conical, u-, j-, i-, y-, inverted y-, and branching.

1.1.2 Burrows and Sediments

Changes in hydrodynamics promote changes in sediment movement about crab burrows. It has been found that more dense assemblages of surficial features may reduce erosion and subsequent redeposition of suspended matter (Friedrichs et al., 2009). The same paper established that high burrow density induced a change in the sediment budget from net erosion to net deposition. Such impacts on local sediment budgets have potentially important implications for managing erosion in the wider region. Near-bed sediment movement may also partly control food availability, which can affect community structure and function (Botto & Iribarne, 2000).

Sediment reworking in two different sediment types has been studied by Needham (2011b) examining the dependence on burrow/crab density, and burrow morphology, maintenance, and turnover. Muddy sediment was found to be more stable than sand, with less reworking occurring and higher burrow longevity. In muddy sediments, erosion rates were reduced in areas with a denser presence of burrows, whereas in sandy sediments, areas with more burrows showed increased erosion rates. The frequency of burrow collapse depends largely on sediment properties, and frequent burrow collapses will increase the amount of mixing occurring within the sediment (Murray et al., 2002). Crab burrows have been shown to trap small particles which are organic matter rich, with the subsequent collapse of the burrows mixing the trapped sediment into the benthos (Botto & Iribarne, 2000). Mixing in this way interrupts the sediments cohesive nature, and

incorporates water into the sediment matrix, and hence affects sediment stability and erodibility (Botto & Iribarne, 2000; Needham et al., 2013).

1.1.3 Burrows and Hydrodynamics

A common behaviour for burrowing organisms is the irrigation of their burrows. Burrow irrigation typically increases flushing rates and reduces residence times for the burrow water. Additionally, irrigation can increase rates of reaction by the introduction of oxygenated water into deeper layers of potentially anoxic sediment (Ziebis et al., 1996; D'Andrea et al., 2002). Whether a burrow has single or multiple burrow openings has been shown to have no significant net effect on tidal flushing capability (Heron & Ridd, 2003), however having multiple loops may increase the entire flushed volume (Heron & Ridd, 2008). Full tidal replacement of burrow water has been observed to occur in mangrove systems over several tidal cycles (Hollins et al., 2009). It has also been shown that presence of waves induces oscillatory flows within empty burrows (Webster, 1992). Computational fluid dynamics have been used to simulate fine scale tidally induced flows through simple u-shaped burrow structures, to find that burrows with multiple loops have longer flushing times (Heron & Ridd, 2001). A study conducted on deposition into pits showed that pits enhanced deposition when flow was considered not fully turbulent (Yager et al., 1993). The same study showed that the aspect ratio of the pit affected the particle concentration within the pit, with the pit collecting less as it grew relatively wider.

Much recent work has considered how above-bed structures protruding into the flow, change hydrodynamics and the subsequent effects of sediment transport and

deposition. It has been shown that in most cases vegetation reduces near-bed flow speeds, creating areas of slow flow where sediment can deposit (Nepf, 2012). In some cases however, the presence of vegetation can induce scour around the bases of the plants (Chen et al., 2012). Vegetation has been shown to create spatial variability and changes in bed stress which also occur where burrows are located (López & García, 1998; Needham et al., 2013). There has been a wealth of literature describing the effect that above-bed structures such as vegetation or mounds have on flow, but less study into the effect that burrows, pits, and tunnels have on near-bed flows.

Burrow building influences solute-surface interactions as burrow tunnels effectively increase the water-sediment boundary surface area (Ziebis et al., 1996; Laverock et al., 2011). The enhanced mixing caused by burrow building increases the rate of exchange between sediment and water. It has also been found that sediment reworking by *austrohelice crassa* increases solute exchange rates considerably (Needham et al., 2011). The resultant deeper mixing also increases sediment permeability (Ridd, 1996). The presence of burrows is also known to alter the boundary layer profile above the sediment (Murray et al., 2002).

A major effect of crab burrowing is increased aeration, as has been shown in studies which explore redox reactions in relation to crab densities. Increased aeration as caused by burrowing crabs has been shown to enhance mangrove productivity in Australia (Smith et al., 1991). Exchanges between anoxic and oxic regions take place in and in close proximity to the burrows (Ziebis et al., 1996; Gilbert et al., 2003; Laverock et al., 2011). Gradients created at the surface-sediment boundary are altered by this bioturbation, increasing remineralisation

rates. Alterations in surface topography caused by burrowing create flows which push oxic water into the sediment, and anoxic water out, which then increases remineralisation of nutrients and metal ions (Ziebis et al., 1996). Larger densities of burrows therefore leads to larger oxygen uptake by the sediment (Ziebis et al., 1996). Previous work in Tairua has focused on the impact that *austrohelice crassa* have on nutrient cycling (Needham, 2011b). Needham et al. (2013) found that mud crabs regulate nutrient cycling, influencing sediment-water interface gradients. Reactions resulting from this modification have potentially significant effects to surrounding biological systems.

1.1.4 Burrows and Nutrients

Wider implications of burrow building may be that crab burrows impact nutrient movement creating a change in nutrient availability and cycling (Gilbert et al., 2003). The processes of nitrification and denitrification have been shown to be both inhibited and enhanced by the presence of burrows, depending on the species involved, burrow placement, or the local environment (Gilbert et al., 1998; Gilbert et al., 2003; Laverock et al., 2011). Increasing the sediment-water interface creates more habitat for microbes which widely control biological processes, such as nitrification and denitrification (Kinoshita et al., 2003; Hollins et al., 2009). Burrow size and spacing were shown to be key factors influencing the stimulation or inhibition of nitrification (Gilbert et al., 2003). The activity depth of biological processes was seen to be a controlling factor in the stimulation of denitrification (Gilbert et al., 1998).

Biota are impacted by burrowing through enhanced mixing of the sediment. This bioturbation increases the mixing of detritus into sediment, increasing the amounts of available nutrients for benthic primary production. As a result of the presence of burrows, primary production and decomposition are both shown to be affected in systems including burrow building species, being enhanced or inhibited depending on the sediment environment (Webb & Eyre, 2004b, 2004a; Tang & Kristensen, 2007; Hollins et al., 2009; Xin et al., 2009; Needham et al., 2013).

1.1.5 Questions Remaining

At the small-scale, the exact nature of burrow building and sediment reworking is yet to be comprehensively physically understood. Flows created by benthic bioturbating fauna have seldom been quantified using high resolution measurements and burrow assemblages and associated rates of sediment disturbance require further quantification. Previous studies have relied upon computational modelling to show small scale processes (Heron & Ridd, 2003; Friedrichs et al., 2009). Other studies have focused on measurement of flows through burrows, with the aim of quantifying flushing rates, however, few studies have focussed on the effect of fine scale flows around burrows on sediment trapping. These limitations may have previously been due to technological inhibitions.

The impacts of these flow alterations may be significant on the ecosystem scale as mud crabs are a ubiquitous species in these soft sediment environments. Having an understanding of how burrow building behaviour differs between environments may assist in the monitoring of organisms which can be linked to long term morphologic change (Snelgrove, 1999). These results will likely provide

insight into the role of burrowing fauna in affecting near-bed flow which will lead to a better understanding of bed shear stress and sediment dynamics, particularly the mobility and retention of fines which, in turn, affects the morphology of estuarine flats. Impacts of this behaviour may be physically significant on larger scales, particularly due to the abundance of bioturbating fauna present in estuaries.

The present study will measure the fine scale physical flows surrounding *austrohelice crassa* burrows in hopes to elucidate how flow is affected by the presence of burrows, and how changes in hydrodynamics may lead to changes in sediment deposition. This study will employ experiments in both field and laboratory settings to quantify the impacts that *austrohelice crassa* have on near-bed flows and sediment trapping.

1.2 Objectives and Aims

This study aims to elucidate the effects of *austrohelice crassa* burrows on near-bed flows and sediment trapping. The following research questions were established to meet this objective:

1) What is the impact of burrow orientation and densities on unidirectional flows?
2) What is the effect of *austrohelice crassa* burrow density on sediment trapping?
3) Can these small scale observations be linked to those made on larger scales?

In particular aims were developed to quantify the influence of *austrohelice crassa* burrows on near-bed flows:

1) Create maps of flows around burrows to: a) identify the impact of burrow orientation on flow, and b) estimate amounts of sediment trapping at various burrow densities.
2) Measure small scale boundary layer flows and calculate turbulent kinetic energy.

Experiments utilised fine scale measurement capabilities, using a Nortek Vectrino Profiler to measure flows surrounding *austrohelice crassa* burrows in a laboratory setting as well as *in situ*. Laboratory experiments explored the impact that a single crab burrows orientation has on near-bed flows. The impact of burrow

density on flows was quantified both in a unidirectional flume, and in the field. Sediment trapping was also quantified in the field.

1.3 Thesis Outline

This thesis begins by introducing factors that affect *austrohelice crassa* burrow distribution, densities, and orientation. Discussion of the possible implications of burrow patterns on sediment budgets, nutrient transport, and benthic interactions follow. Justification for the need for research into the impacts of crab burrows on benthic flows is established. An aim is developed, followed by the objectives of this thesis. In Chapter 2 the methodologies undertaken to elucidate the impacts of *austrohelice crassa* burrows on near-bed flows are described. This thesis includes two major sections of experimentation; laboratory experiments, and field experiments. The methodologies and results of each are described separately. Finally, in Chapters 3 and 4 comparisons and discussion are made regarding the nature and impacts of flows around *austrohelice crassa* burrows.

CHAPTER TWO: METHODOLOGY

Two approaches were taken to determine the influences of crab burrow densities on near-bed flows: laboratory, and field experiments.

2.1 Laboratory Experiments

Two separate sets of laboratory experiments were conducted with the aim of determining: 1) the influence of crab burrow orientation on benthic flows using a single artificial crab burrow, and 2) the influence of multiple crab burrows upon near-bed flows using an artificial crab burrow array.

2.1.1 Flow Flume

All laboratory experiments were conducted in a recirculating flume in the Benthic Flow Laboratory at the University of Waikato, which has been previously described by Miller et al. (2002). The flume has inner dimensions of 7.9 m long, 0.5 m wide, and 0.5 m depth, and consists of acrylic casing with a 0.4 m diameter return pipe below (Figure 2). A propeller driven by an AC motor was fixed at the downstream end, and used to vary the flow speeds within the flume. The flume floor was smooth apart from a working area 6.45 m from the upstream end. The working area consisted of a recess filled with sand into which single burrows or an array could be inserted. The flume was filled with fresh water to a depth of 0.15 m. The tank was seeded with powdered limestone seeding material which has been shown to provide sufficient backscatters to ensure high measurement coherence for the acoustic instrument (Lohrmann & Nylund, 2008).

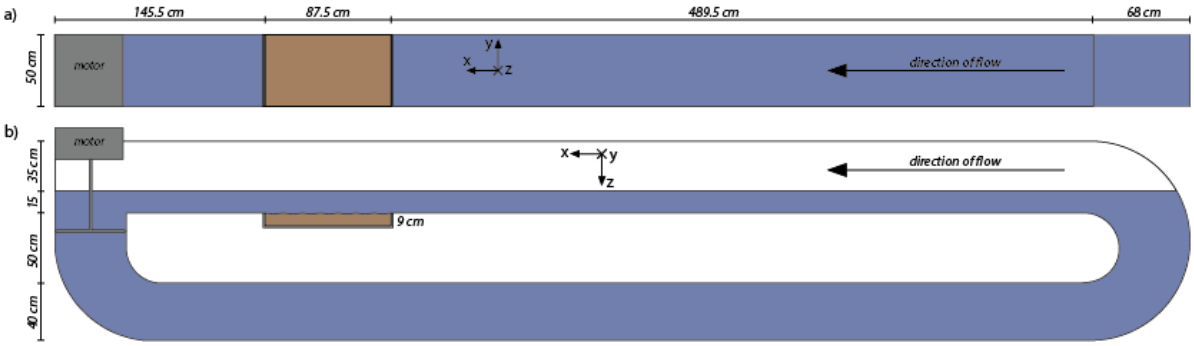

Figure 1: Diagram of the flume showing the working area (brown) where (a) top view, and (b) side view.

2.1.2 Individual Burrow

The first experiment involved measurement of flows around a single burrow in various orientations to discern whether burrow orientation affects flow. A single burrow was created from polyvinyl chloride piping (Figure 3). The burrow had an internal diameter of 2 cm, and was 18 cm long. The burrow was created to mimic the most frequently encountered burrow shapes previously reported by Needham et al. (2010).

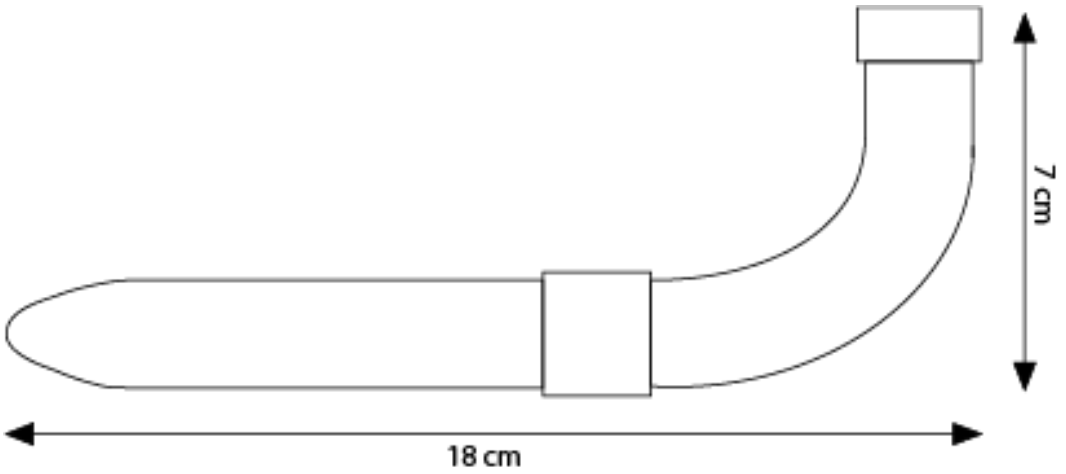

Figure 3: Schematic of the individual burrow inserted into the bed array.

The measurement area was divided into three equal sections, with the central and upstream sections filled with medium size sand (~500 µm), collected from the field site and sieved to remove the small sized fines which would potentially resuspend under the flow speeds used and cause scour around the burrow. The downstream panel was covered with an acrylic insert. The burrow was placed close to the centre of the measurement area to lessen edge effects from the tank to sand transition and tank walls (Figure 4).

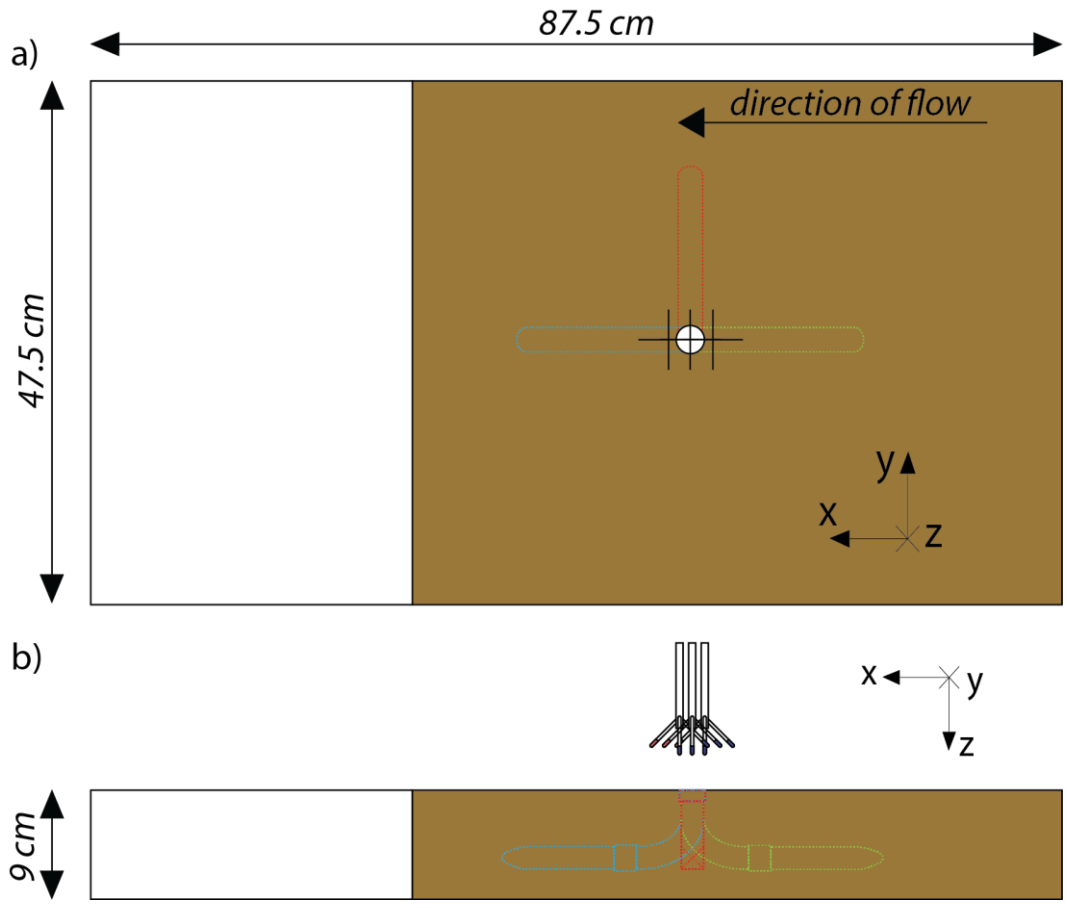

Figure 4: Single burrow within measurement area, showing the three measurement positions of the Vectrino, and the three different burrow orientations (blue = 0°, red = 90°, green = 180°), where a) top view, and b) side view. The brown and white areas represent sand (57.3 cm long) and plastic (29.2 cm long) inserts, respectively.

A series of flow measurements were made using a Nortek Vectrino Profiler Acoustic Doppler Velocimeter (Figure 5). Measurements of three components of velocity (x,y,z) were taken over a profiles with 1 mm depth increments from 0.35 to 0.7 cm from the central transducer of the instrument which was placed 60 mm above the bed. Measurement runs included three positions of the Vectrino profiler: upstream, directly above, and downstream of the burrow opening. The upstream and downstream measurements were taken with the probe very near to the corresponding edges of the burrow opening. Each position was sampled for one minute at a sampling rate of 50 Hz.

Figure 5: Probe end of the Nortek Vectrino Profiler Acoustic Doppler Velocimeter used for all experiments. The red tine indicates the x flow direction.

The burrow was placed within the measurement area at three different orientations (Figure 6). For the upstream and downstream positions the profiler was placed above the outside edge of the burrow.

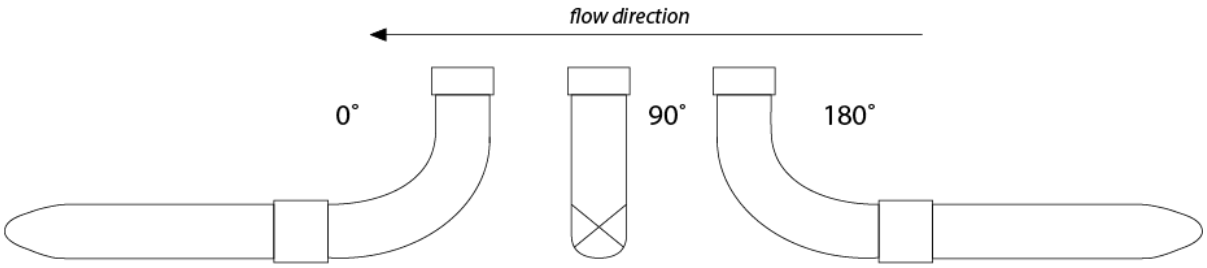

Figure 6: Burrow orientations within the tank.

Five different speeds were used at each burrow/velocimeter position, with increments of 1 Hz of input forcing from the AC motor corresponding to approximately 1 cm/s flow speed (Table 1).

Table 1: Laboratory runs in the unidirectional flume for a single burrow.

Set	Position relative to burrow	Orientation (°)	Speeds (cm/s)	Records
1	Above	0, 90, 180	1, 2, 5, 7, 10	1-15
2	Upstream	0, 90, 180	1, 2, 5, 7, 10	16-30
3	Downstream	0, 90, 180	1, 2, 5, 7, 10	31-45

2.1.3 Burrow Array

The second experiment used an artificial burrow array to determine the influence of burrow density on near-bed flows. An array of identical artificial burrows (as used in the first experiment) was created (Figure 7). Burrows were randomly secured to a 47 cm wide and 60 cm long plastic hatching at random locations to create a maximum density of 74 burrows/m^2. The range of burrow densities used was similar to natural burrow densities observed in the field by Needham et al. (2010) who reported densities varying from 207 burrows/m^2 in mud

30.7 burrows/m^2 observed in sand. In Pepe Inlet however, the highest burrow density observed was 63 burrows/m^2. For both practical reasons, and since both the flume sediment and the sediment in the field were identified as being medium-coarse sand, the range of densities created for the artificial array did not extend to 207 burrows/m^2.

Flow measurements were taken using a Nortek Vectrino Profiler Acoustic Doppler Velocimeter carefully placed at 6 cm from the bed measuring at 50 Hz, taking one minute of data at each position for each treatment. For each array and flow speed, twenty positions were selected using a random number generator to give co-ordinate positions. Each position lay within a measurement area of 18 cm by 37 cm situated 5 cm from the array edges, in the downstream portion of the array (Figure 8). When a position was determined above a burrow, the co-ordinate was discarded and another taken until 20 positions directly above the sediment were determined within the area.

Figure 7: Crab burrow array in flume before burial showing positions of artificial burrows. Flow direction is from right to left.

For each array, six speeds were induced (approx. 1 cm/s, 2 cm/s, 5 cm/s, 7 cm/s, 10 cm/s, 15 cm/s) using an AC motor attached to a propeller. These speeds were chosen to reflect typical flow speeds found within tidal flats. The flow in the flume remained less than the erosion threshold during all runs. The Vectrino Profiler captured one minute of data at 50 Hz at each position.

Once all flow speeds and positions had been sampled for an array, burrows were randomly removed in groups of five as seen in Figure 8. Measurements were repeated as before, to give a range of decreasing burrow densities. All experiments are summarised in Table 2.

Table 2: Summary of runs performed in the unidirectional flume with varying densities.

Set	Density (burrows/m^2)	Number of replicates	Speeds (cm/s)	Records
1	0	20	1, 2, 5, 7, 10, 15	1-120
2	7	20	1, 2, 5, 7, 10, 15	121-240
3	18	20	1, 2, 5, 7, 10, 15	241-360
4	29	20	1, 2, 5, 7, 10, 15	361-480
5	40	20	1, 2, 5, 7, 10, 15	481-600
6	52	20	1, 2, 5, 7, 10, 15	601-720
7	63	20	1, 2, 5, 7, 10, 15	721-840
8	74	20	1, 2, 5, 7, 10, 15	841-960

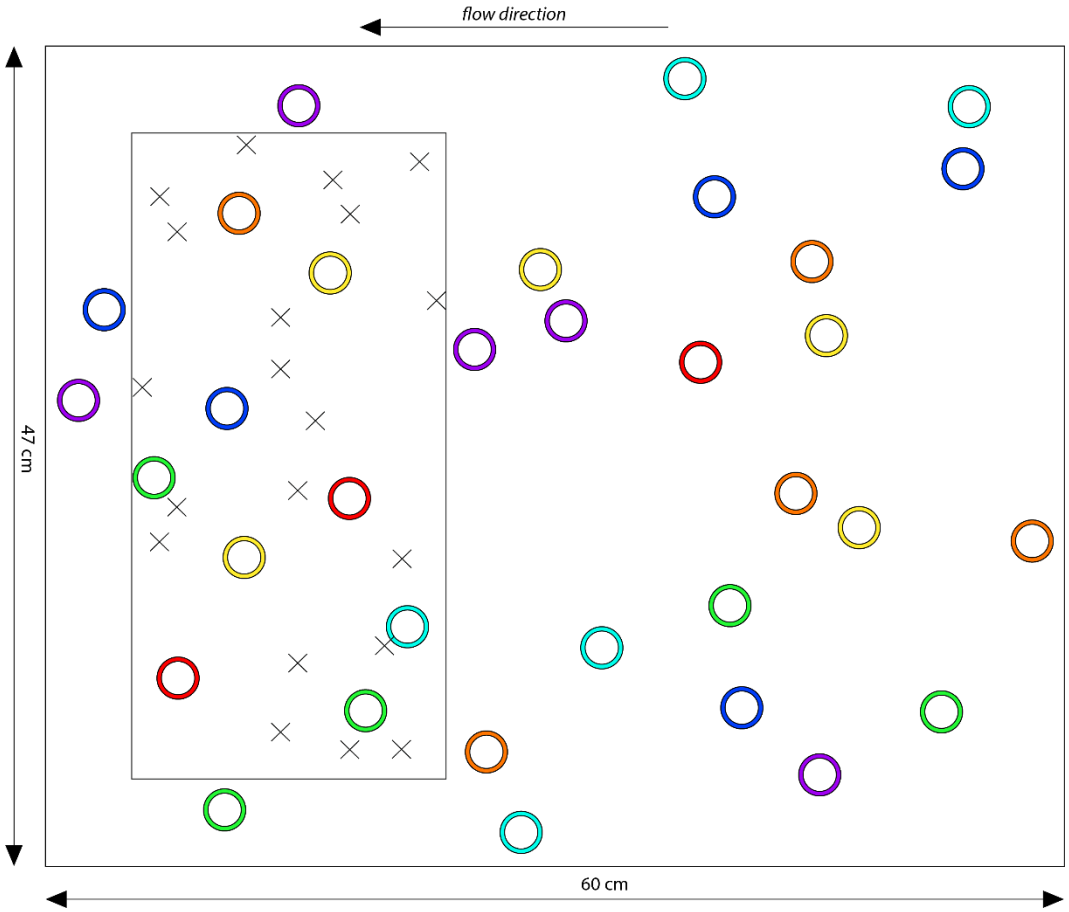

Figure 8: Diagram of the working area of the flume. Burrow positions are colour coded to the order in which they were removed (purple = 1st removal, cyan = 2nd removal, blue = 3rd removal, green = 5th removal, yellow = 6th removal, and red = 7th removal). Crosses indicate measurement locations.

2.1.4 Data Analysis

A quality check was run to remove all data with low correlation (< 70%) values. The individual burrow experiment data was also run through a script to remove any phase wrapping (Lhermitte & Serafin, 1984; Lohrmann et al., 1990). Velocities (u, v, w, corresponding to along, across channel, and vertically, respectively) were time averaged over the record length (~60 s) to give mean

velocities ($\bar{u}, \bar{v}, \bar{w}$). For the array data, turbulent kinetic energy (TKE) was calculated for each record using

$$TKE = \frac{1}{2}\rho(\bar{u}'^2 + \bar{v}'^2 + \bar{w}'^2),$$

where u', v', w' are instantaneous velocity fluctuations (ie: $u' = u - \bar{u}$), and ρ(=1000 kgm^{-3}) is the water density. Mean speeds over time were calculated for each run using

$$mean\ speed = \sqrt{\bar{u}^2 + \bar{v}^2}\ .$$

TKE were normalised for each position as

$$normTKE = \frac{1}{\rho} \times \frac{TKE\ at\ each\ position}{mean\ speed\ at\ zero\ burrow\ density\ at\ each\ position^2}\ .$$

The flume burrow array data were normalised as above to minimise the effect of horizontal flow variation in the flow flume.

2.2 Field Experiments

2.2.1 Site Description

Tairua is a settlement located on the eastern side of the Coromandel Peninsula, North Island, New Zealand (Figure 9). Tairua town is located on the northern end of the Tairua Harbour entrance, with Pauanui on the south. The estuary has an area of approximately 6 km^2 and is barrier enclosed (Liu, 2014). Tairua Estuary was formed following the Holocene marine transgression approximately 8000 years ago when sea level rose and stabilised, flooding the Tairua River valley. The estuary inlet has a 130 m wide main channel with a 4 m maximum depth (Liu, 2014). Tairua Estuary is classed as a tidally-dominated, partially-mixed estuary (Liu, 2014) and flows within the estuary are ebb dominant (faster ebb tidal currents than flood). The estuary is meso-tidal (tidal range of 1.63 m), with 77 % of the harbour area being intertidal (Hume & Herdendorf, 1992). It is estimated that the tidal exchange of estuarine water with the open coast is high, with 82 % of each incoming flood tide being coastal water (Bell, 1994). Within the estuary are tidal flats consisting of sandy to sandy-muddy sediment (Needham et al., 2013). The sedimentation rate within the estuary has been quantified as 6 mm yr^{-1} on the tidal flats, with rates as high as 22 mm yr^{-1} in the harbour entrance (Liu, 2014).

2.2.2 Study Sites

Field experiments were undertaken over two days in July within Pepe Inlet located in the Tairua Estuary on the Coromandel Peninsula, Waikato (Figure 9). The first experiment involved the measurement of flows around arrays of natural crab burrows, varying in density. Three Vectrino Profilers were placed in the centre

of crab burrow arrays (Table 3). The profilers were placed only in points not directly above crab burrow entrances. Frames were hammered into the sediment beside the crab burrow array to hold the profilers. Care was taken to leave the measurement area free of disturbance via human contact. The Vectrino Profilers were set up 5-6 cm from the sediment surface so that a full boundary layer profile may be observable, with the x direction probe always pointing north. The bed position was obtained from the median bottom distance measured by the central transducer. The sites were chosen to be of similar tidal level, slope, and sediment type. Burrow density of each site was characterised using a 1 m^2 quadrat roughly centred on the Vectrino measurement location.

Table 3: Summary of the field experiments and instrumentation locations.

Site		Burrow Density	GPS Co-ordinates		Sediment Type	Distance above surface (cm)
Burrow Type	Density Treatment		Latitude (S)	Longitude (E)		
Natural	Dense	62	-37.00249703	175.845460	Fine Sand	5.2
	Sparse	30	-37.00268101	175.845825	Fine Sand	5.5
	Control	0	-37.00242100	175.845932	Fine Sand	6.0
Artificial	Dense	74	-37.00254103	175.846872	Fine Sand	5.7
	Sparse	40	-37.00250499	175.846848	Fine Sand	5.7
	Control	0	-37.00248102	175.846811	Fine Sand	5.7
	ADCP	0	-37.00242402	175.846776	Fine Sand	N/A

For the second experiment, two of the artificial burrow arrays (74 burrows/m^2 and 40 burrows/m^2) from the laboratory experiment were buried in the sediment at Pepe Inlet. A third site, containing no burrows, was selected and

disturbed similarly to act as a procedural control. The experimental areas containing no crabs, and the comparative artificial burrow arrays were chosen to be as similar as possible. Sites were relatively near enough to comparable hydrodynamic conditions whilst being far enough from each other to rule out edge and disturbance effects. The Vectrino Profilers were placed in a position to capture both the incoming and outgoing tides without disturbance from the instrument frames. The burrow arrays were placed with the incoming tidal flow entering from the south-southeastern direction. A Nortek Aquadopp Acoustic Doppler Current Profiler (ADCP) was also set up for the second experiment in line with the artificial array experimental sites and used to provide pressure measurements at 8 Hz.

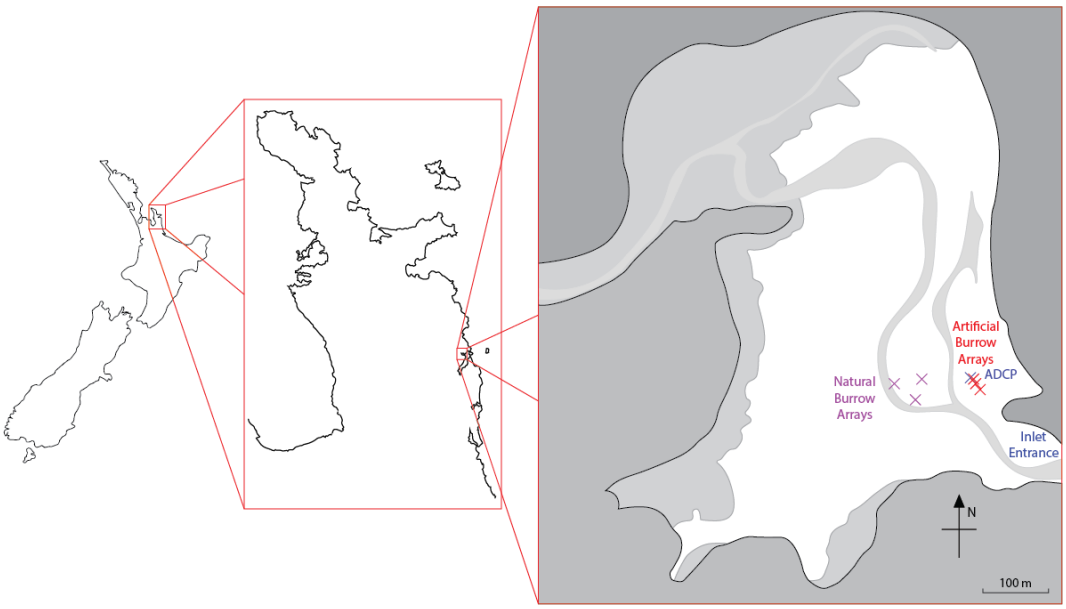

Figure 9: Site map of Pepe Inlet in Tairua Harbour, Coromandel, New Zealand. Red crosses show Vectrino Profiler positions above artificial crab burrows. Magenta crosses show Vectrino Profiler positions above natural crab burrows. The blue cross shows the location of the ADCP.

Figure 10: Artificial burrow arrays. Front-back: control, sparse, and dense arrays buried in the sediment. Arrows indicate the incoming tidal flow direction.

During burial of the arrays, care was taken to ensure that the artificial burrow edges remained flush with the sediment surface (Figure 11). Sediment was prevented from entering the burrows during installation. The arrays were filled with seawater and plugged before being left for one tidal cycle to settle into the sediment. The arrays were then checked and bungs carefully removed to ensure no intrusion of sediment had occurred before measurement.

a)

b)

Figure 11: Buried dense burrow array with bungs inserted (a), and after bung removal (b).

Sediment grab samples were taken from all sites following measurement. Samples were taken from the surface (down to 2 cm) of sediment from a 1 m^2 quadrat around the profiler location at each site.

2.2.3 Measurements

For both experiments, the Vectrino Profilers collected burst samples of 10 minute lengths over a tidal cycle. The data was manually filtered to remove periods of time where the flow was considered too wavy. A quality check was run to remove all data with low correlation values (where correlation < 70%). The data was then analysed as above in section 2.1.4.

2.2.4 Sediment Analysis

Subsamples from the sediment grab samples from each field site were digested in 10 % hydrogen peroxide to remove organic matter (Day, 1965). The samples were then run through the Malvern Mastersizer 2000 to obtain sediment grain sizes. The median grain sizes are reported here.

The burrow sediment samples were analysed using total suspended solids methods described in Franson (1998). The samples were agitated and 20 ml poured onto pre-weighed and dried filter papers within a vacuum apparatus. The samples were rinsed through, until the filter papers were dry enough to remove. The papers were then dried in an oven at 105°C for 24 hours. The dried filter papers were then weighed and the total suspended sediment content calculated using:

$$\frac{mg\ total\ suspended\ solids}{L} = \frac{(A - B) \times 1000}{sample\ volume, ml}$$

where A = weight of filter + dried sediment in mg, and B = weight of the dried filter in mg (Franson, 1998). Within each array an average suspended sediment concentration was found. The average suspended sediment contents were then

converted using the average burrow volume (40 ml) to find the average sediment caught (g, and kg) per area (m^2, and km^2).

CHAPTER THREE: RESULTS

3.1 Laboratory Experiments - Individual Burrow

In general, the laboratory data for the individual burrow experiments was of high quality (Figure 12a) with correlations consistently over 90 %, where coherence above 70 % are considered satisfactory (Rusello, 2009), with the largest flow speeds being in the along-flume (u) direction (Figure 12c, Figure 13a) which also had the relatively smallest variation. Across flume and vertical velocities showed larger relative variation, with a time-averaged flow speed of approximately zero from measurements at the centre of the tank. Measurements taken from the centre of the tank over a sandy bed (x = 58.3, y =23.8) show a characteristic logarithmic flow profile in the along-flume direction and no mean flow in the across-flume and vertical directions (Figure 13a-c). However, flow within the tank exhibited substantial variations owing to imperfections in the tank and pump system. Instantaneous profiles of vertical, across-flume, and along-flume speeds show the variable nature of the v, and w components of velocity (Figure 13c-e).

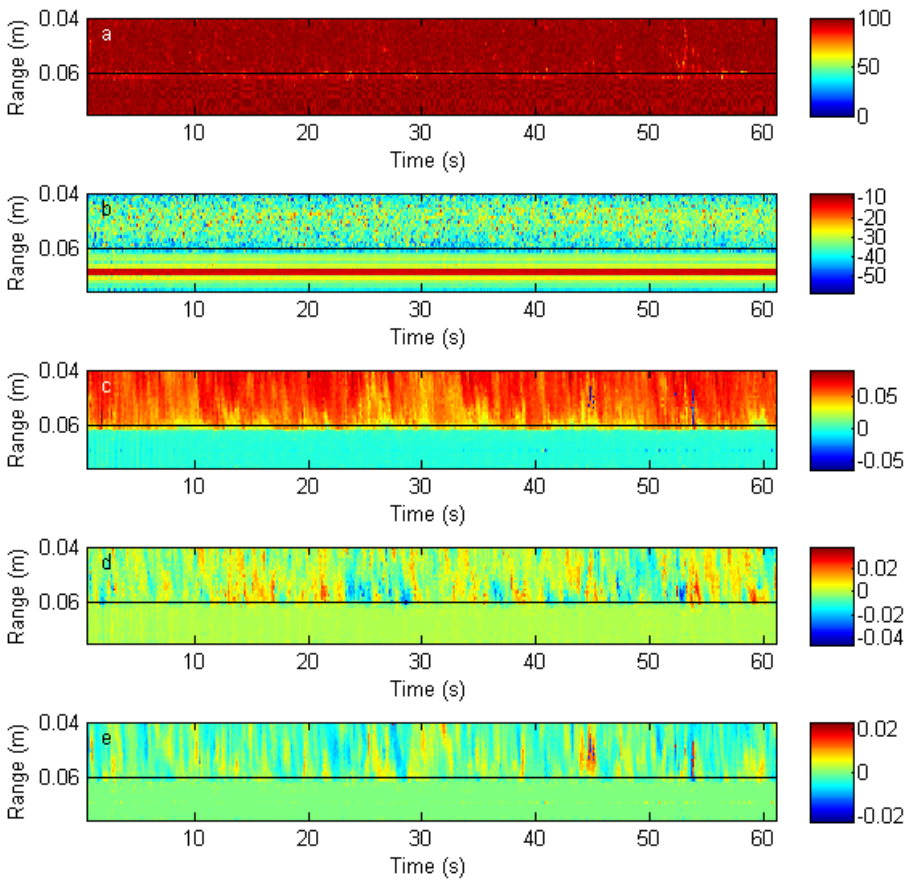

Figure 12: Raw data plots for when the burrow was at 0° to the flow showing correlation (%)(a), backscatter (dB)(b), u, v, and w velocities (m/s)(c-e). The black line shows the tank bottom.

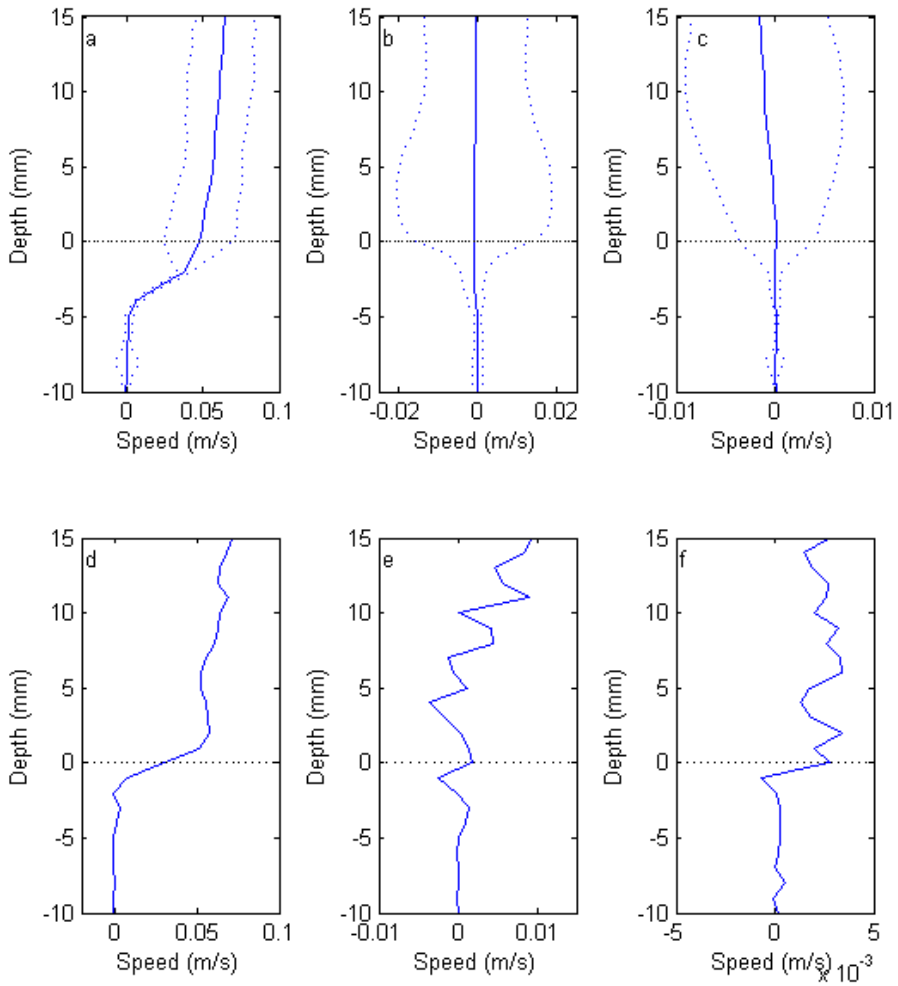

Figure 13: Time-averaged profiles of near-bed u, v, and w velocities (a-c), with variance bounds shown as dotted lines and instantaneous profiles for when the burrow was at 0° to the flow of velocities (d-f: u, v, and w velocities). The dotted black line shows the bed bottom.

With no burrow inserted into the sand, the along-flume velocity showed a fairly typical boundary layer profile, having a sharp decrease in velocity near to the bed, with a gradual increase in flow speed toward the top of the profiles (Figure 14). The Vectrino Profiler was carefully positioned directly above the burrow opening to give an indication of whether flows are penetrating down into the burrows. When a single burrow was inserted into the sediment, velocities remained above zero for at least a few millimetres into the burrow, producing slightly modified boundary layer

profiles, with a more gradual decrease in flow speed toward the bottom of the profile (Figure 15).

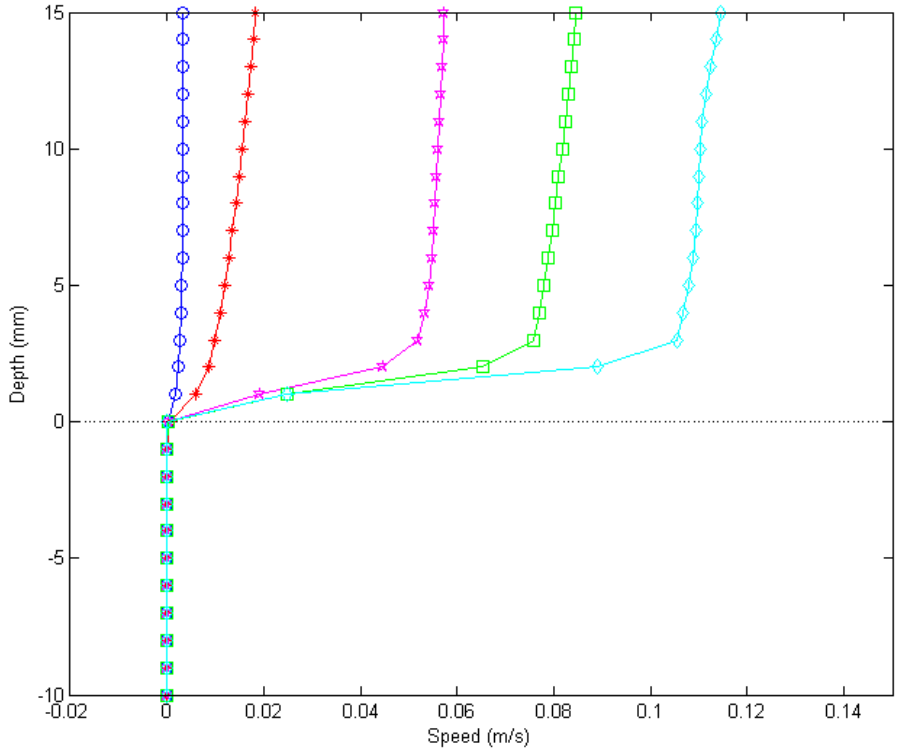

Figure 14: Profiles of time-averaged (over one minute) u component of velocity within the flume when no burrow was present. The colours/symbols (blue/circles, red/asterisks, pink/stars, green/squares, and cyan/diamonds) indicate the five different pump settings that were used corresponding to horizontal velocities of roughly 1, 2, 5, 7, and 10 cm/s, respectively. The dashed line indicates the bed surface.

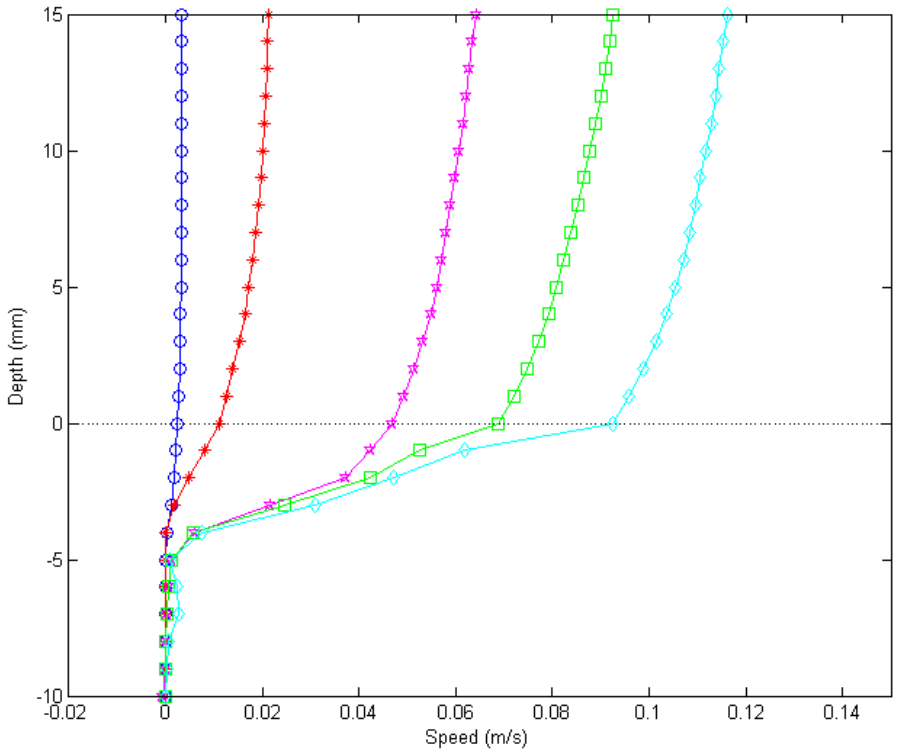

Figure 15: Profiles of time-averaged (over one minute) u component of velocity within the flume when a burrow was placed into the sediment at an angle of 0° to the flow direction and measurements taken from directly above. The colours/symbols (blue/circles, red/asterisks, pink/stars, green/squares, and cyan/diamonds) indicate the five different pump settings that were used corresponding to horizontal velocities of roughly 1, 2, 5, 7, and 10 cm/s, respectively. The dashed line indicates the bed surface.

When the burrow was rotated by 90° to the flow direction, the profiles were slightly modified relative to the no burrow case, with flows extending into the burrow a small way. However, flows with the burrow at 90° weren't as strong or penetrated as deep as the 0° case, with a sharper rate of decrease in velocity within the burrow (Figure 16). When the burrow was rotated by 180° to the flow direction, the profiles showed modification, and the boundary layer flows extended slightly further into the burrow (Figure 17). As flow extends further into the burrow, the

speeds above the bed are larger for when the burrow is at 0°, and lesser for when the burrow is at 90° and 180° (Figure 18).

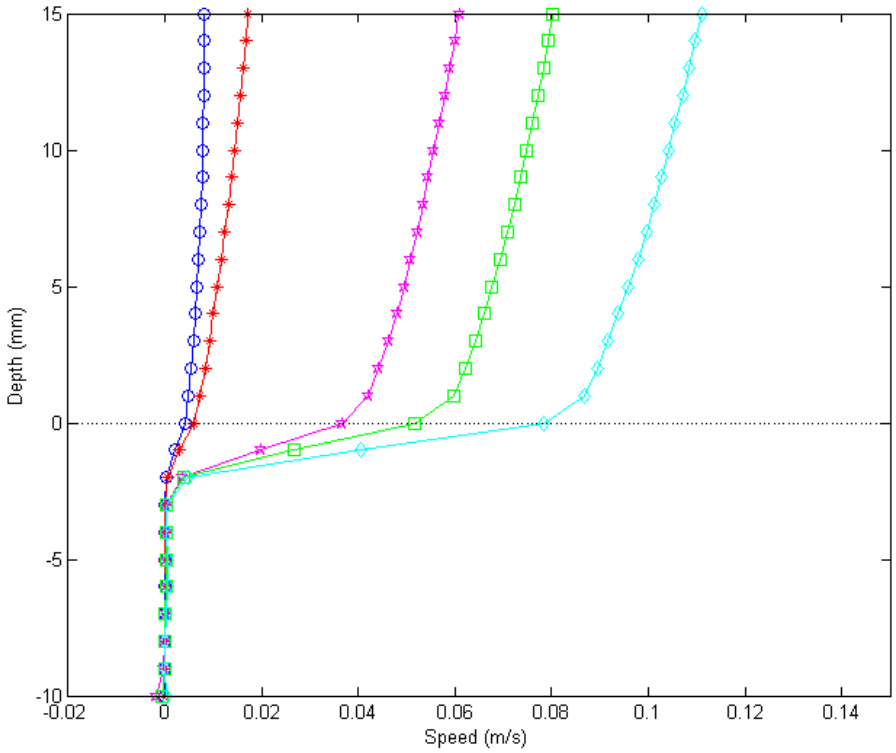

Figure 16: Profiles of time-averaged (over one minute) u component of velocity within the flume when a burrow was placed into the sediment at an angle of 90° to the flow direction and measurements taken from directly above. The colours/symbols (blue/circles, red/asterisks, pink/stars, green/squares, and cyan/diamonds) indicate the five different pump settings that were used corresponding to horizontal velocities of roughly 1, 2, 5, 7, and 10 cm/s, respectively. The dashed line indicates the bed surface.

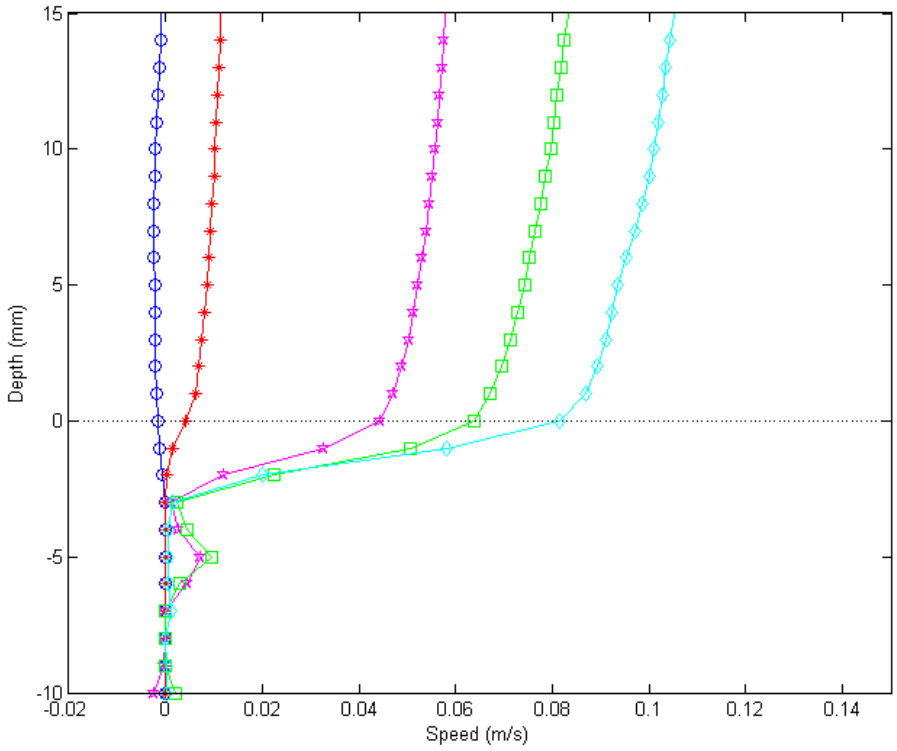

Figure 17: Profiles of time-averaged (over one minute) u component of velocity within the flume when a burrow was placed into the sediment at an angle of 180° to the flow direction and measurements taken from directly above. The colours/symbols (blue/circles, red/asterisks, pink/stars, green/squares, and cyan/diamonds) indicate the five different pump settings that were used corresponding to horizontal velocities of roughly 1, 2, 5, 7, and 10 cm/s, respectively. The dashed line indicates the bed surface.

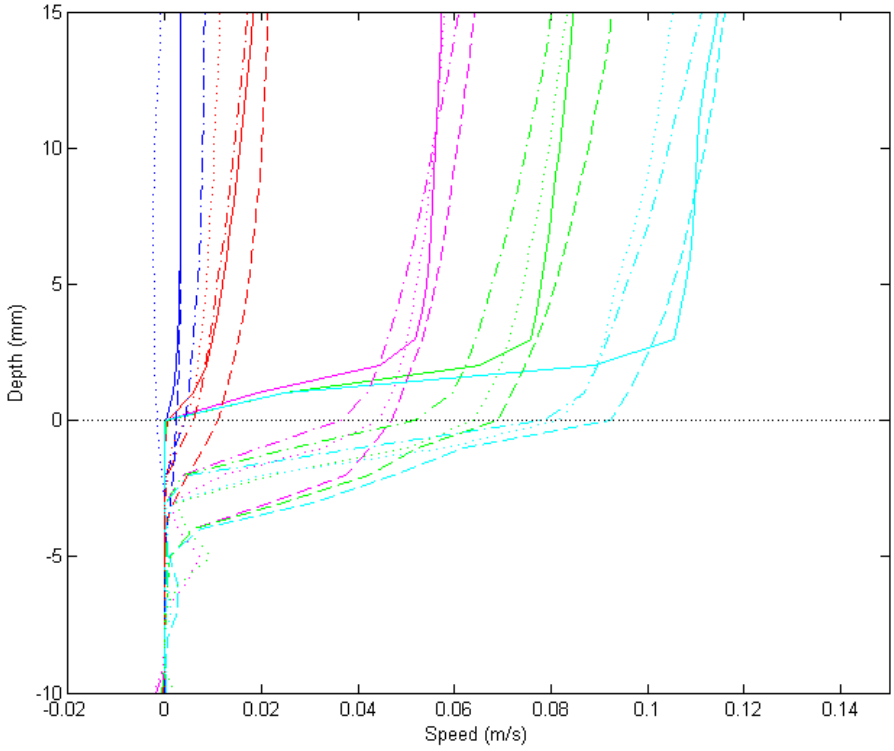

Figure 18: Differences between along-flume velocities for all orientation treatments. The colours (blue, red, pink, green, and cyan) indicate the five different pump settings that were used corresponding to horizontal velocities of roughly 1, 2, 5, 7, and 10 cm/s, respectively. The line styles (solid, dashed, dash-dotted, and dotted) correspond to the treatments, respectively (no burrow, burrow at 0°, 90°, 180°). The black dashed line indicates the bed level.

Profiles captured from above, slightly upstream, and slightly downstream of the burrow showed a slight difference in along-channel flow speeds when forced at 2, 5, or 7 cm/s (Figure 19, Figure 20, Figure 21). Differences between the upstream, above, and downstream profiles were most evident when the burrow was at 0°, with the downstream profile apparently extending farther into the burrow. Generally, the upstream flows are not affected (ie, the flow is supercritical) but downstream the flows sped up when the burrow was at 0°.

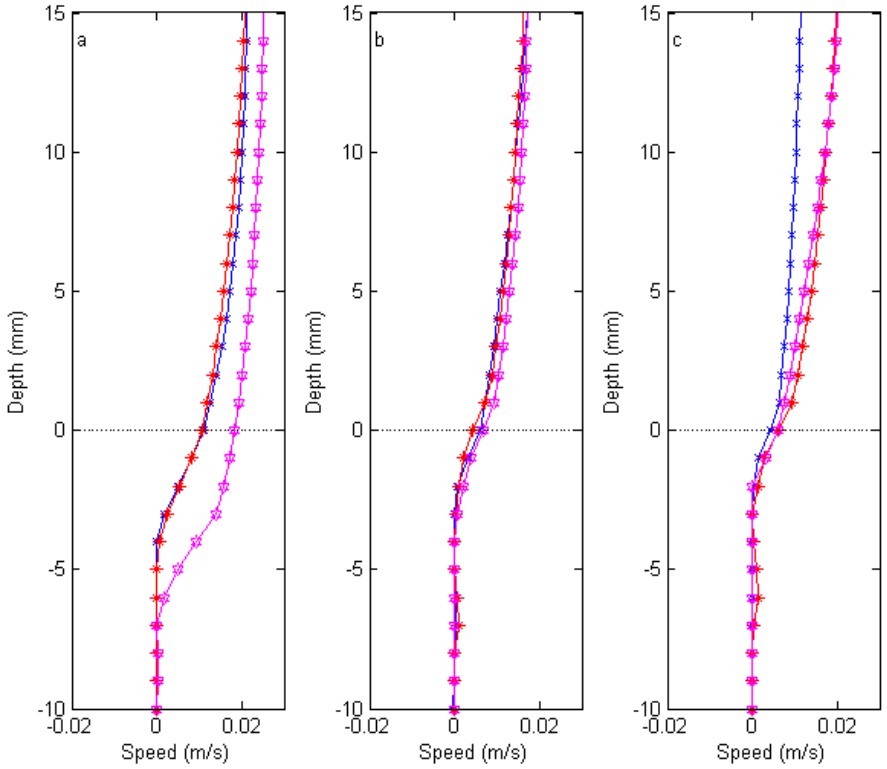

Figure 19: Comparison of profiles of mean along-flume speeds collected above (blue), slightly upstream (red), and slightly downstream (pink) of the burrow at the 0° (a), 90° (b), and 180° (c) positions, with a forced flow speed of 2 cm/s.

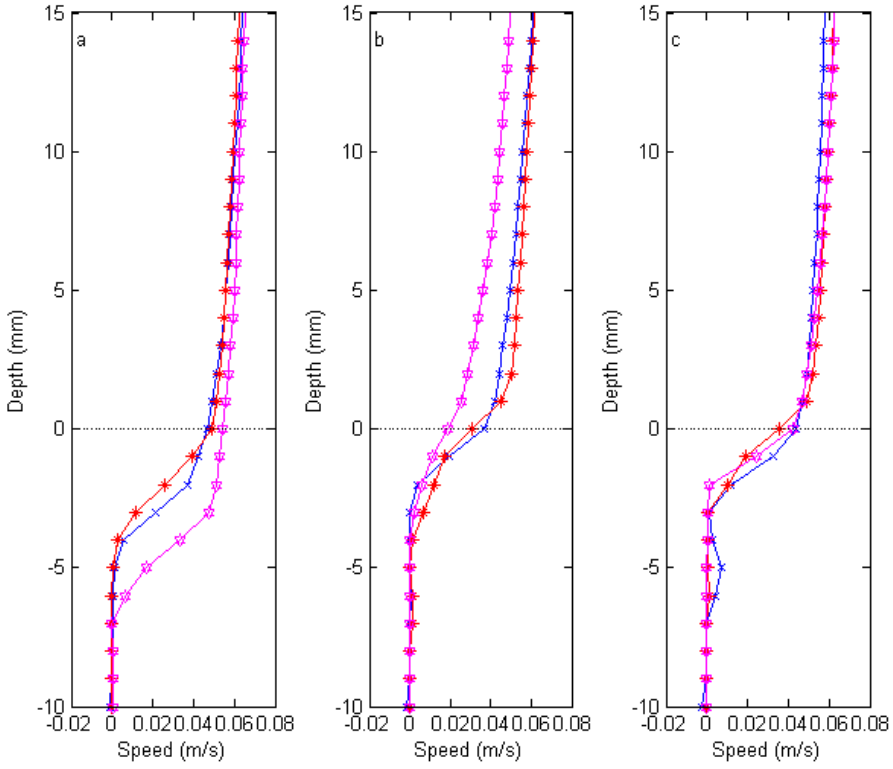

Figure 20: Comparison of profiles of mean along-flume speeds collected above (blue), slightly upstream (red), and slightly downstream (pink) of the burrow at the 0° (a), 90° (b), and 180° (c) positions, with a forced flow speed of 5 cm/s.

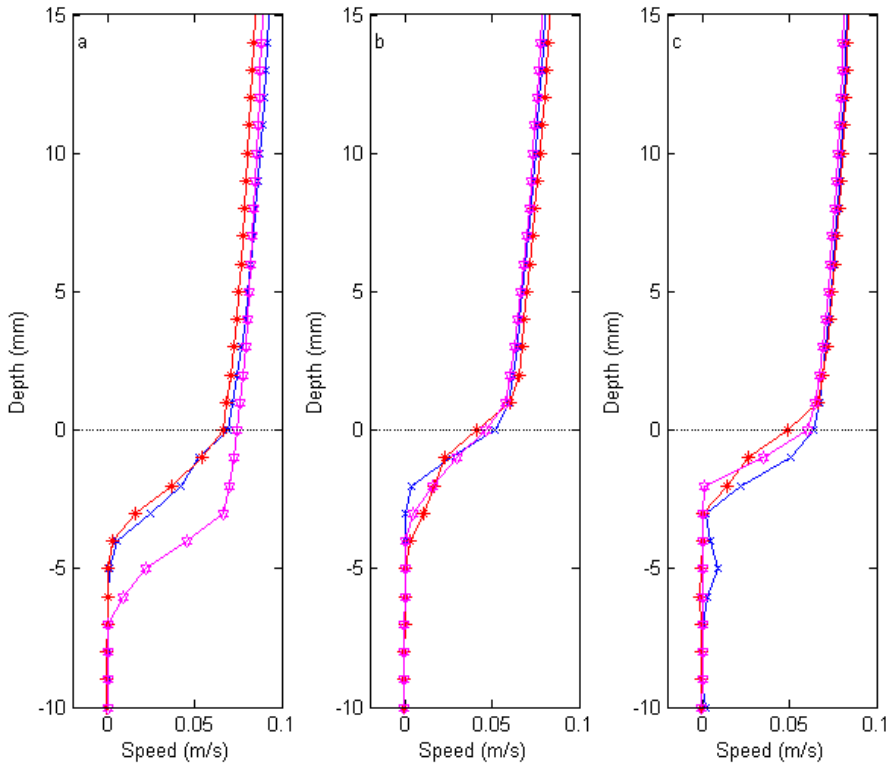

Figure 21: Comparison of profiles of mean along-flume speeds collected above (blue), slightly upstream (red), and slightly downstream (pink) of the burrow at the 0° (a), 90° (b), and 180° (c) positions, with a forced flow speed of 7 cm/s.

Overall, the presence of burrows appeared to alter the along-flume-direction profiles only slightly. Differences in the v velocity component were more pronounced between treatments, but of smaller overall magnitudes, and were not deemed significant.

3.2 Laboratory Experiments - Burrow Array

Data taken from the burrow array experiments showed high correlation, and the highest velocities with the smallest variation in the along-flume direction (Figure 22). Across flume and vertical velocities showed larger relative variation, but with a time-averaged flow speed of approximately zero (Figure 23). The time-averaged TKE profiles all followed a similar shape, with a sharp increase in TKE near the bottom, a slight peak at the top of the boundary layer, followed by a tapering off to a steady value reaching up into the free-stream consistent with uniform flow speeds observed in the mean flow (Figure 24).

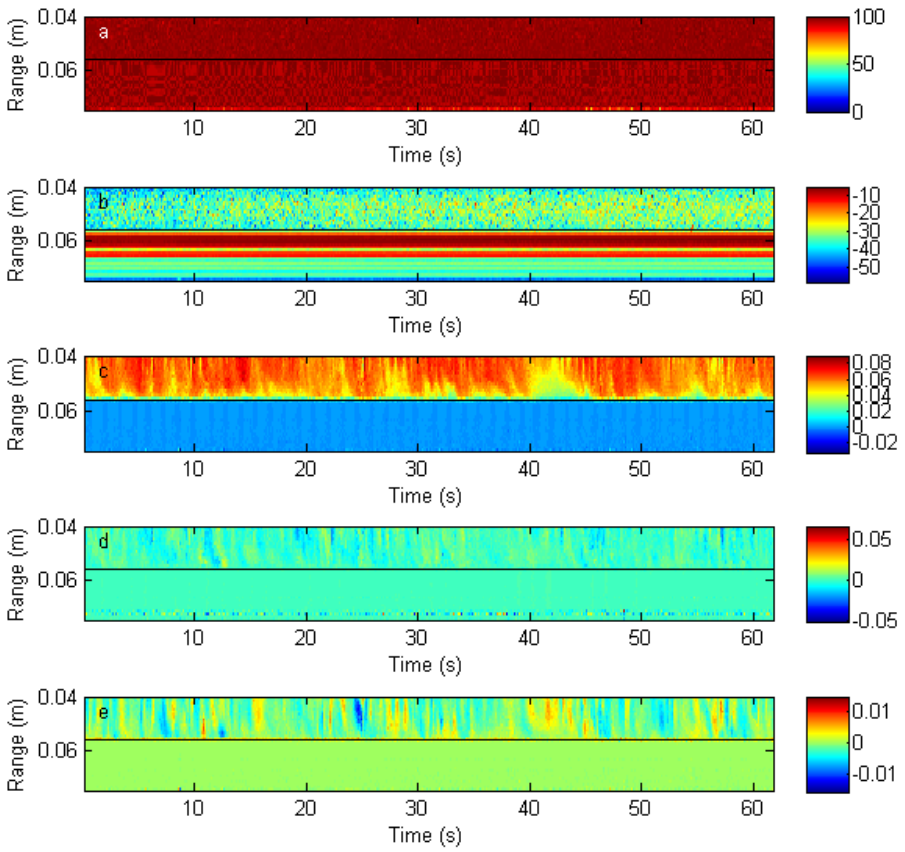

Figure 22: Raw data plots for when the Vectrino Profiler was at position x=12, y=6 showing correlation (%)(a), backscatter (dB)(b), u, v, and w velocities (m/s)(c-e). The black line shows the level of the seabed.

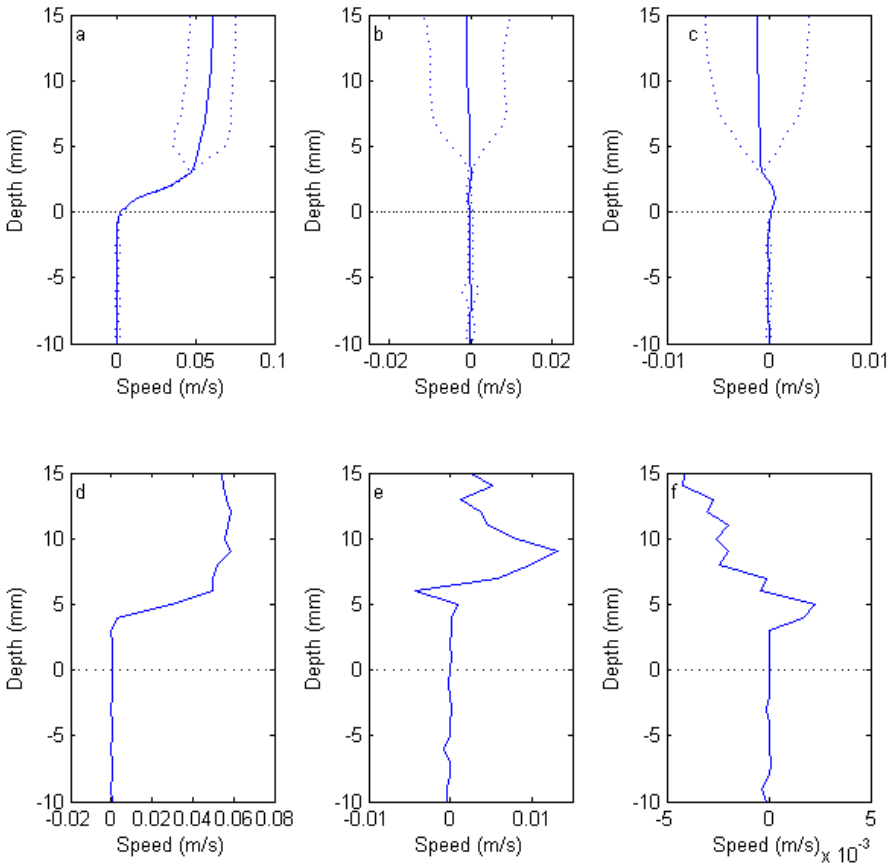

Figure 23: Instantaneous profiles for when the Vectrino Profiler was at position x=12, y=6 showing velocities (d-f: u, v, and w velocities), time-averaged profiles of near-bed velocities (bottom, left to right, u, v, and w velocities), with variance bounds shown as dotted lines.

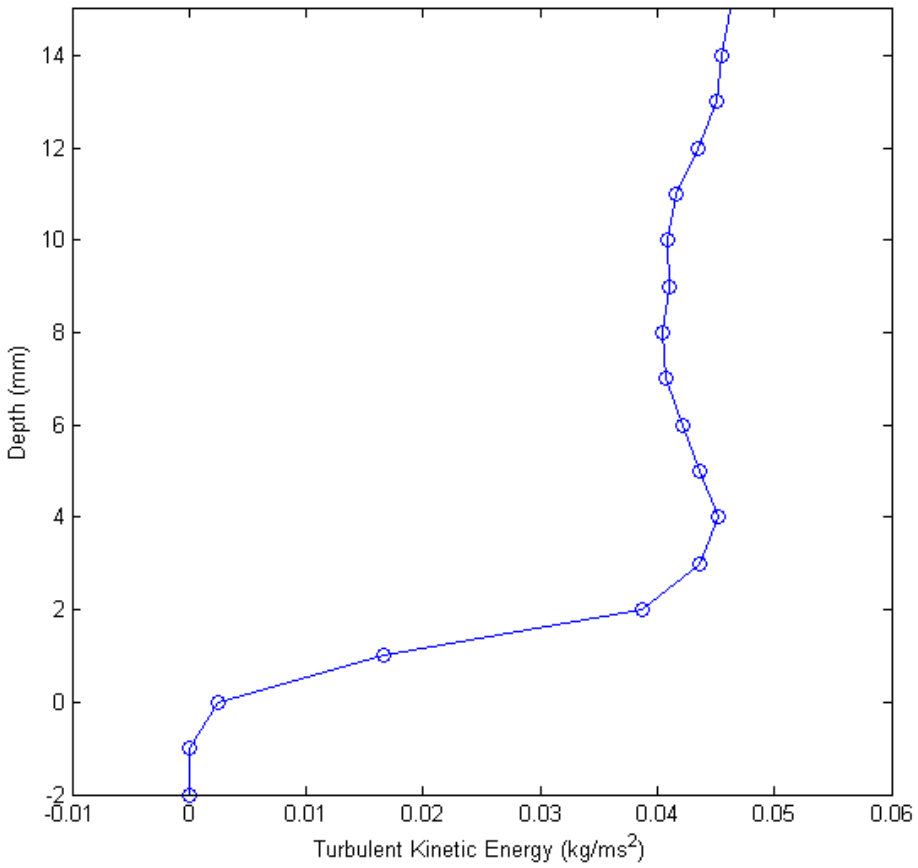

Figure 24: Time-averaged profile of TKE when the Vectrino was in the first position (x = 12, y = 6), at a burrow density of 74 burrows/m^2, and flow speed was approximately 5 cm/s.

The effect of burrow density on flow was quantified in terms of turbulent kinetic energy (TKE), calculated from the three components of velocity (u, v, and w). At all densities the TKE increased with flow speed, non-linearly (Figure 25).

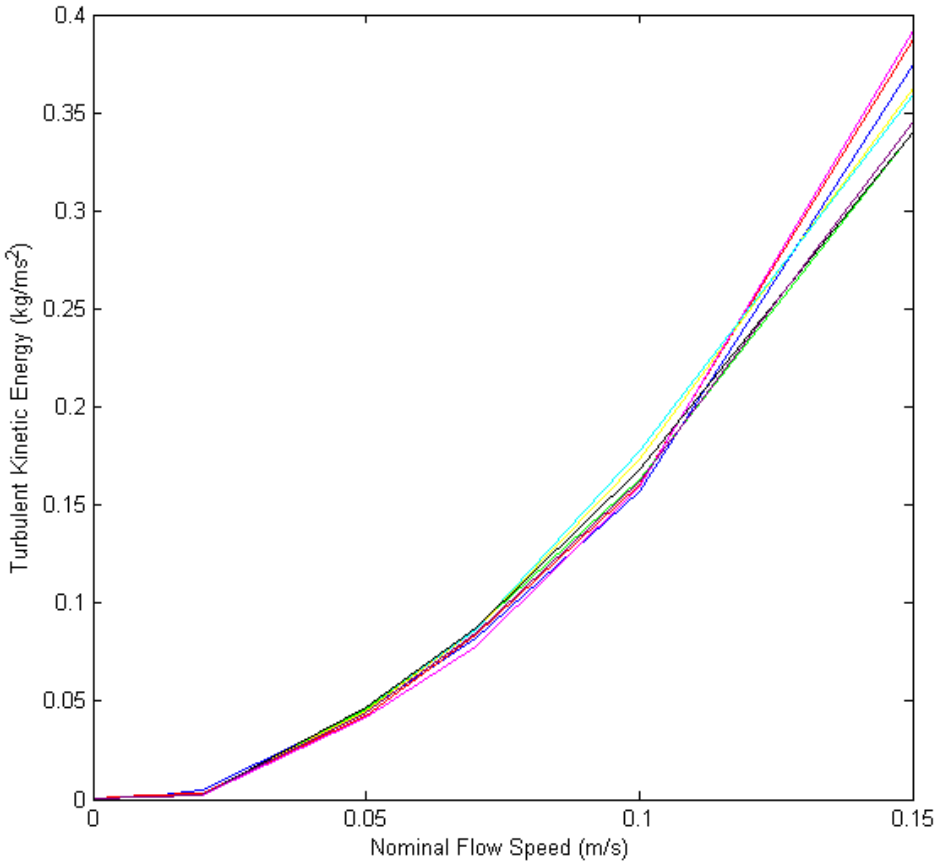

Figure 25: Turbulent kinetic energy increases with increasing flow speed. Colours (blue, red, green, yellow, pink, cyan, black, and purple) indicate the different burrow densities (0, 7, 18, 29, 40, 52, 63, and 74 burrows/m^2, respectively).

The time-averaged and depth-averaged TKE calculated over entire profiles ($z > 0$) showed that, as expected, for higher flow speeds the TKE was higher (Figure 26).

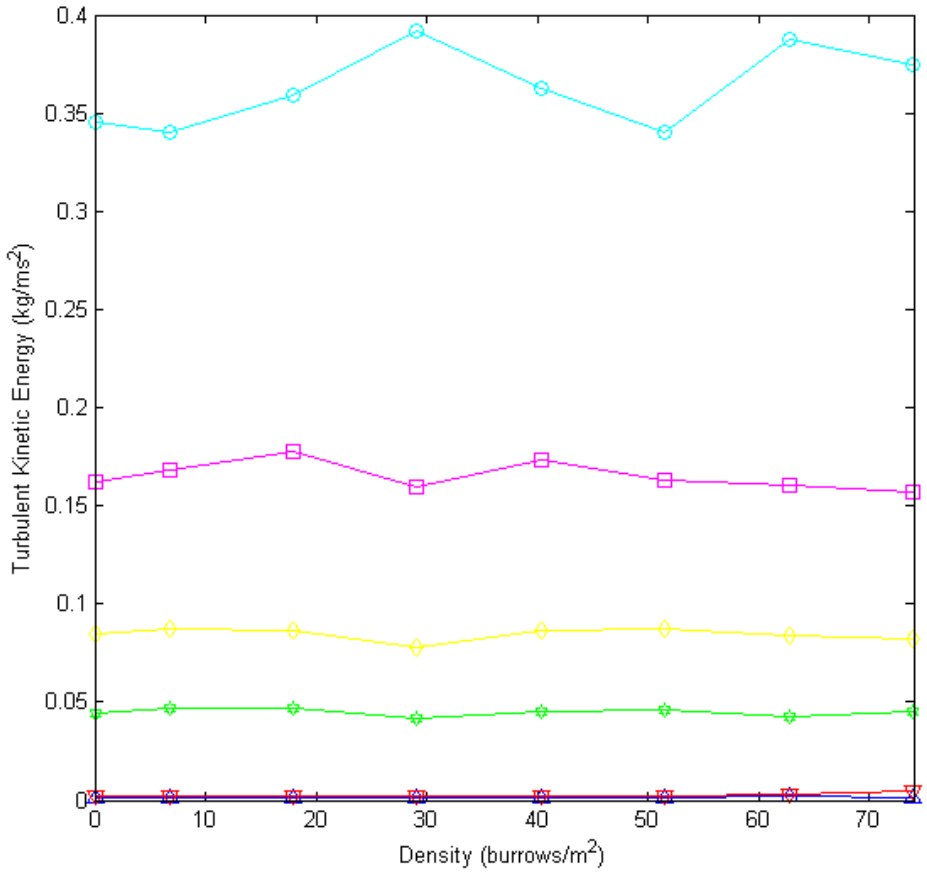

Figure 26: Burrow density (burrows/m^2) against depth-averaged turbulent kinetic energy (TKE) at six flow speeds in the flume. The colours/markers (blue/triangles, red/upside-down triangles, green/stars, yellow/diamonds, pink/squares, and cyan/circles) indicate the different flow speeds (1, 2, 5, 7, 10, and 15 cm/s, respectively).

The data over the full range of speeds shows that, as expected, the TKE increases with flow speed non-linearly. A peak (at 30 burrows per m^2) and following decrease of TKE with increasing burrow density was shown. The data were normalised (as above in methods 2.1.4) to remove dependence on flow speed and the effect of flow variations within the flow flume (Figure 27). Normalising the data at each location by the control density (0) at each position revealed a difference in flow regimes between the higher flow speeds (7 cm/s, 10 cm/s, 15 cm/s) and lower flow speeds (1 cm/s, 2 cm/s, 5 cm/s). For the lower speeds, a peak TKE at

approximately 30 burrows/m^2 can be seen in Figure 26, followed by a gradual decrease in TKE with increasing burrow density. A linear trendline fitted to the low flow speed data (1, 2, and 5 cm/s) showed a general decreasing trend of TKE with increasing burrow density, although there exists significant scatter.

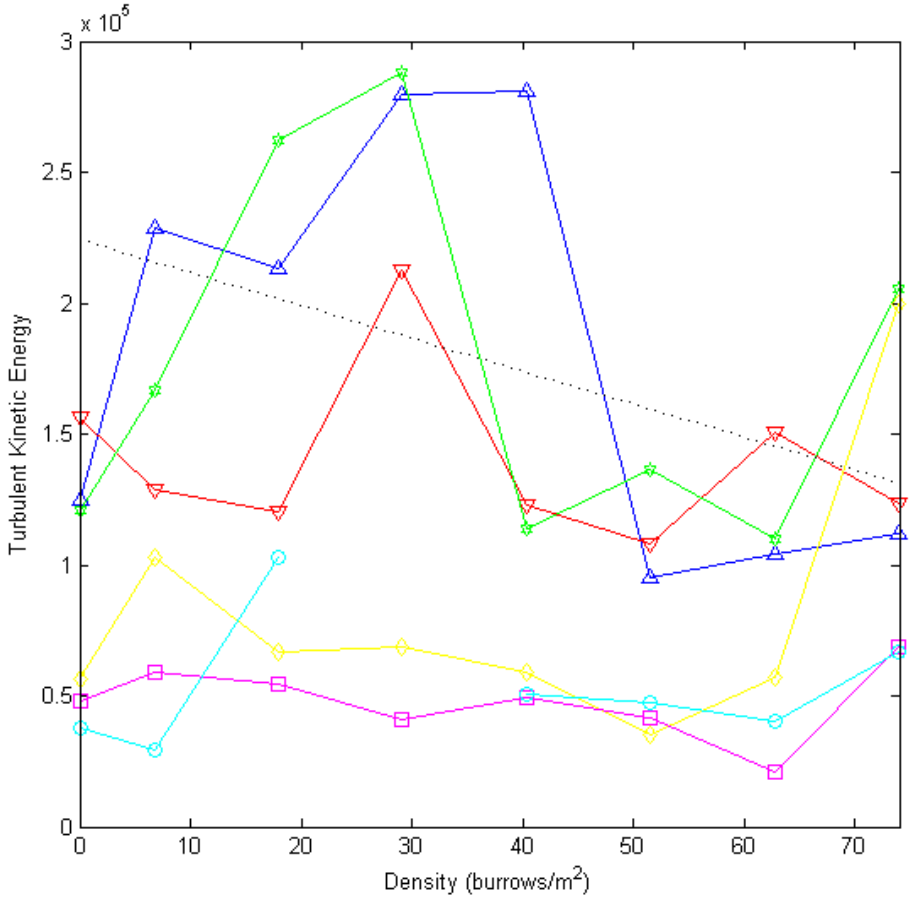

Figure 27: Burrow density (burrows/m^2) vs. mean normalised turbulent kinetic energy (TKE) at six flow speeds in the flow flume normalised by the mean speed of the control density at each position squared. The colours/markers (blue/triangles, red/upside-down triangles, green/stars, yellow/diamonds, pink/squares, and cyan/circles indicate the different flow speeds (1, 2, 5, 7, 10, and 15 cm/s, respectively). The dotted line indicates a linear trendline showing the decrease in TKE with increasing burrow density for the lower flow speeds (1, 2, and 5 cm/s).

Although subtle, this decrease in TKE for higher burrow densities may indicate that the flow has transitioned, and may indicate the transition to more of a skimming flow regime in which the ‘holes’/burrows are seen as an enhanced roughness element rather than single obstructions. At the higher flow speeds (yellow, pink, turquoise) this decrease is not observed, with higher TKE for larger burrow densities. There is however a slight increase in TKE among the higher flow speeds at the highest burrow density. This increase may indicate a potential for a flow regime change with larger densities (not reached here).

.

3.3 Field Experiments

3.3.1 Environmental Conditions - Hydrodynamics

The experiments were conducted on the 9th and 10th of July, 2015 during the austral winter. Both days were moderately windy for the majority of the measurement period, creating surface waves in the Pepe Inlet where the experiments took place. High tide occurred at approximately 1300 h on the 9th and at 1400 on the 10th. The estuary is ebb dominant, and consequently the ebb and flood flows varied in duration.

Observations made by the ADCP used for the pressure sensor which was placed in line with the artificial burrow arrays on the second day of measurement showed a significant wave height of approximately 0.035 m and a period (T) of around 0.9 s.

3.3.2 Environmental Conditions - Sediments

The grab samples taken from the field were all of similar distribution and size, being classed as fine sand on the Wentworth Scale (Figure 28). These samples were only slightly less coarse than the sediment used in the laboratory flume experiments, which was classed as coarse-medium sand (~500 µm).

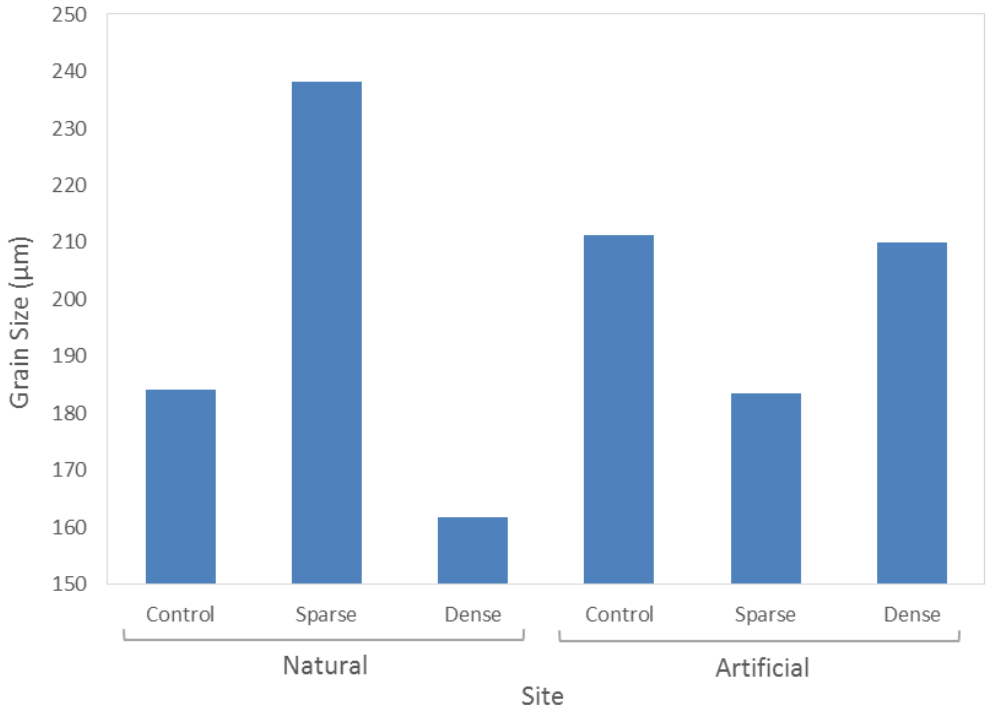

Figure 28: Mean grain sizes for the sediment grab samples taken from the six measurement sites in the field.

3.3.3 Natural and Artificial Burrow Arrays

During the experiment, windy conditions created waves of sufficient height for orbital velocities to reach the sea bed. Times of relative calm conditions were selected manually in order to allow for comparison with laboratory data (Figure 29).

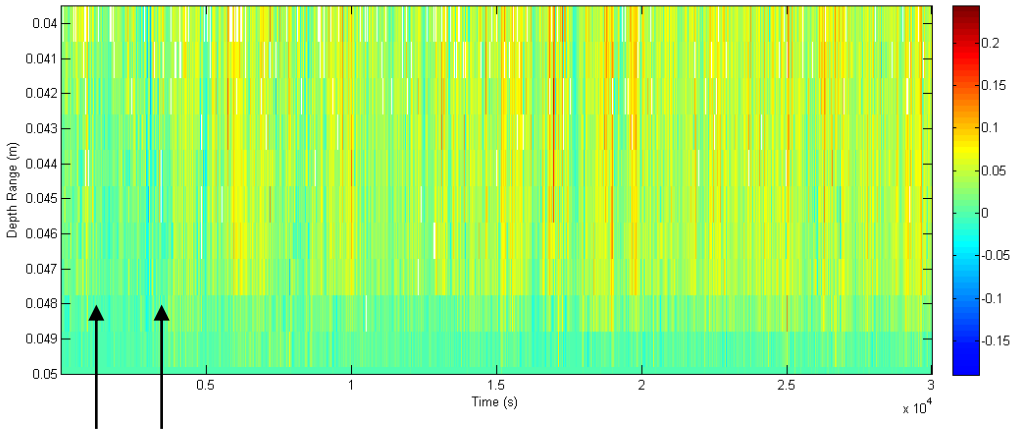

Figure 29: Raw field data for x-direction velocity, indicating times of low waves selected for comparison. White areas indicate bad data which was removed.

The field experiments using the artificial burrow arrays exhibited a similar trend to that observed in laboratory experiments of increasing TKE with increasing burrow density up until 40 burrows/m^2 followed by a decrease in TKE with increasing burrow density (Figure 30). These data were normalised to allow clearer comparison between densities (Figure 31). The pattern of increase and decrease was similar to that found in the laboratory array experiment for intermediate flow speeds, suggesting the potential development of skimming flow at higher burrow densities.

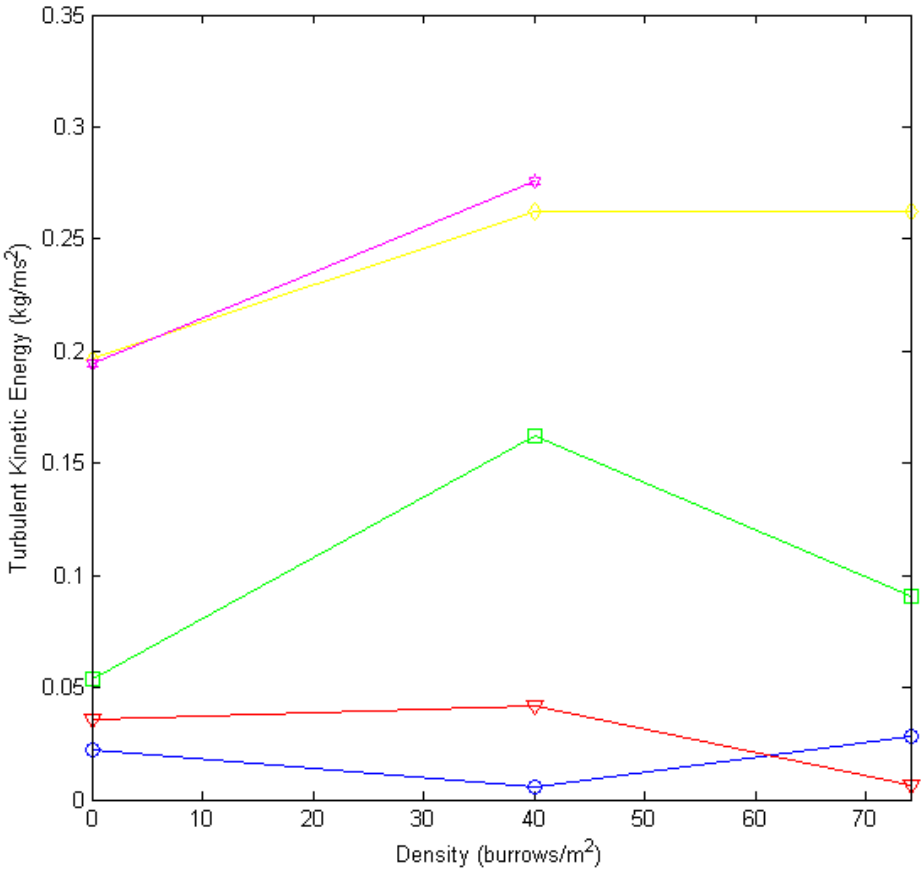

Figure 30: Burrow density (burrows/m^2) vs. mean turbulent kinetic energy (TKE) at six flow speeds measured above the artificial burrow arrays and procedural control (0 burrows) in the field. Colours/markers (blue/circles, red/triangles, green/squares, yellow/diamonds, and pink/stars) indicate nominal flow speeds of around 1, 2, 5, 7, and 10 cm/s

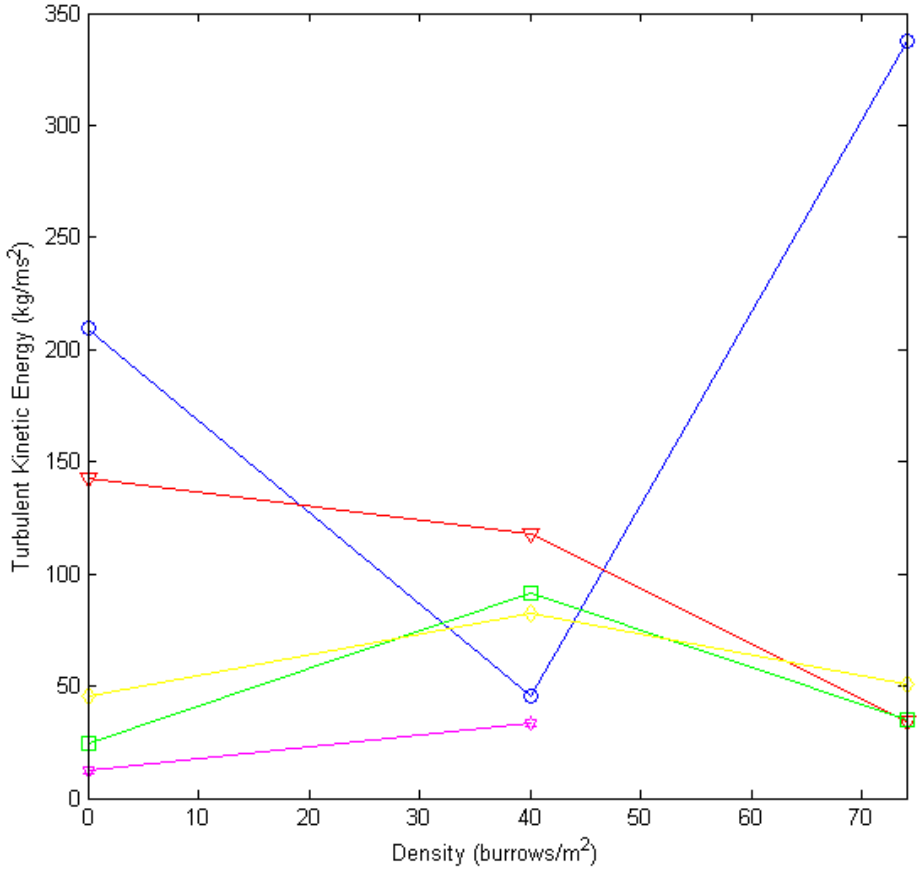

Figure 31: Normalised data of burrow density (burrows/m^2) vs. mean turbulent kinetic energy (TKE) at six flow speeds measured above the artificial burrow arrays and procedural control (0 burrows) in the field. Colours/markers (blue/circles, red/triangles, green/squares, yellow/diamonds, and pink/stars) indicate nominal flow speeds of around 1, 2, 5, 7, and 10 cm/s.

In the natural crab burrow array experiments, TKE clearly increased with increasing burrow density for all flow speeds with strong dependence on burrow densities (larger relative increases) for the three lower flow speeds, similar to the pattern that was found in the laboratory experiments (Figure 32). The normalised data show the pattern of increasing TKE with increasing burrow density more clearly (Figure 33). In these arrays there was no evidence of skimming flow developing, as TKE continued to increase. The discrepancy for the 1 cm/s flow

speed may have been because of remaining wave action, as the waves could not be fully removed from the data.

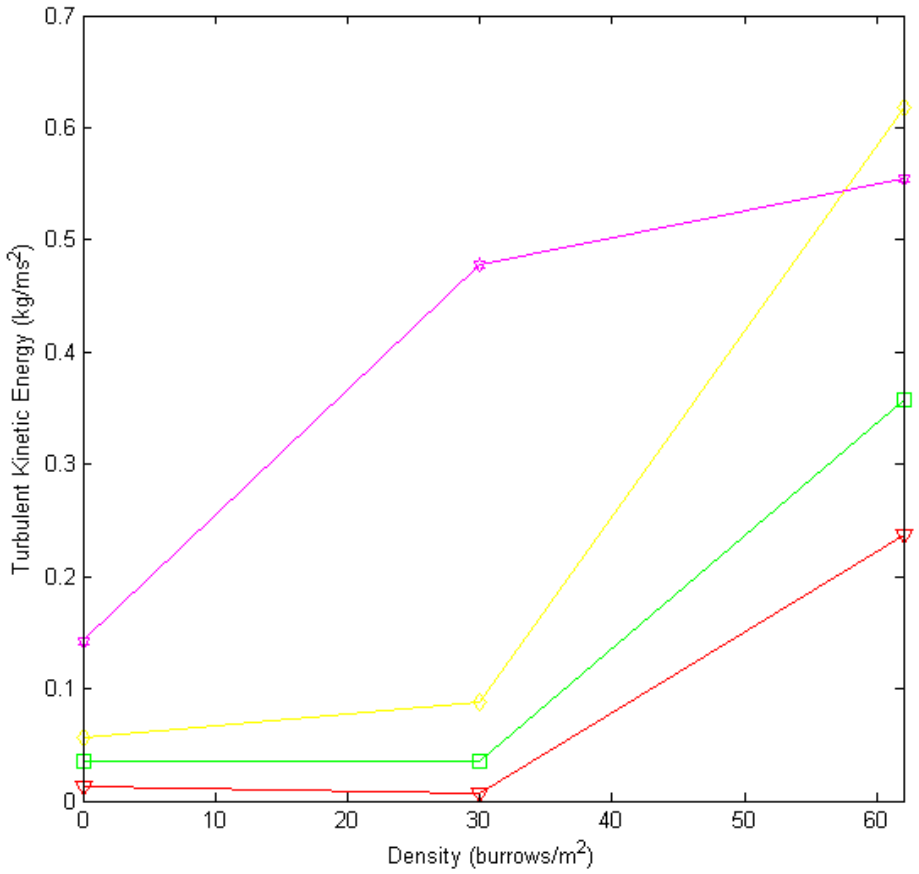

Figure 32: Burrow density (burrows/m^2) vs. mean turbulent kinetic energy (TKE) at four flow speeds measured above the natural burrow arrays and control (0 burrows) in the field. Colours/markers (red/triangles, green/squares, yellow/diamonds, and pink/stars) indicate nominal flow speeds of around 2, 5, 7, and 10 cm/s.

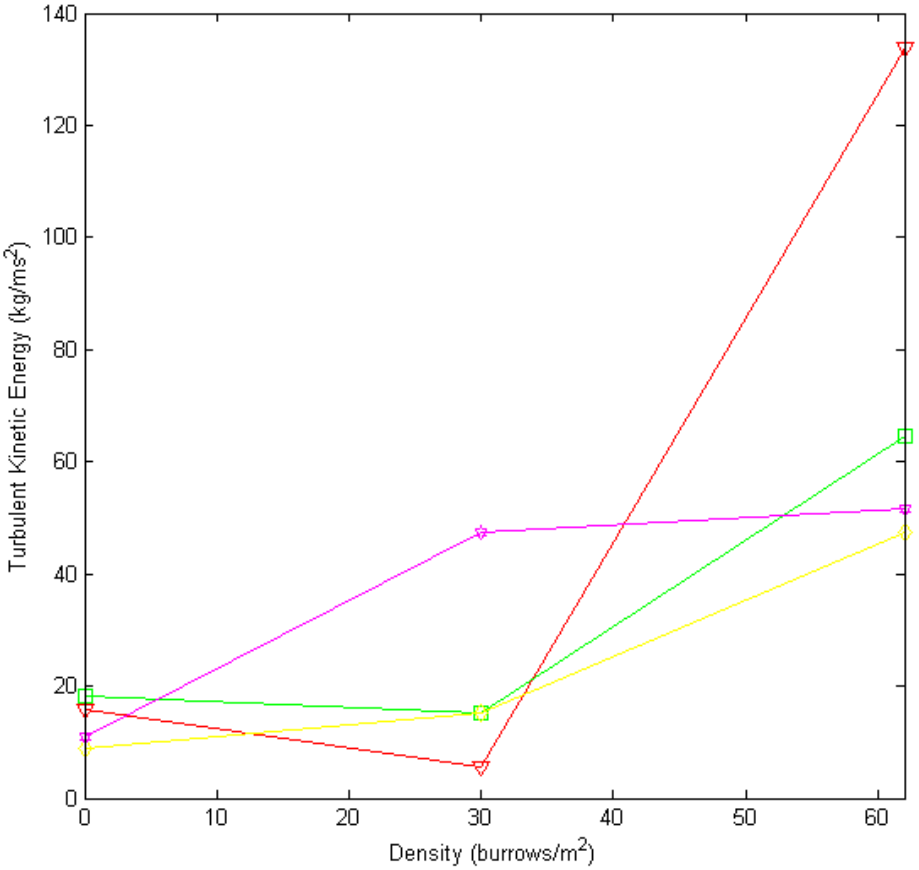

Figure 33: Normalised data of burrow density (burrows/m^2) vs. mean turbulent kinetic energy (TKE) at four flow speeds measured above the natural burrow arrays and control (0 burrows) in the field. Colours/markers (red/triangles, green/squares, yellow/diamonds, and pink/stars) indicate nominal flow speeds of around 2, 5, 7, and 10 cm/s.

Combining the field results from both artificial and natural burrows, demonstrates an increase of TKE with burrow densities up to 62 burrows/m^2, followed by a decrease at the largest burrow density, suggesting that skimming flow occurs (Figure 34). Transition to skimming flow in the field experiments may occur at higher densities than in the laboratory experiment. It may also be that in the slightly muddier sediment, which typically houses higher densities of crab burrows, the transition occurs later on. The normalised data (Figure 35) from all field

experiments again shows different modes of behaviour between high flow speeds (pink), and lower flow speeds (red, green, and yellow), similar to that found in the laboratory.

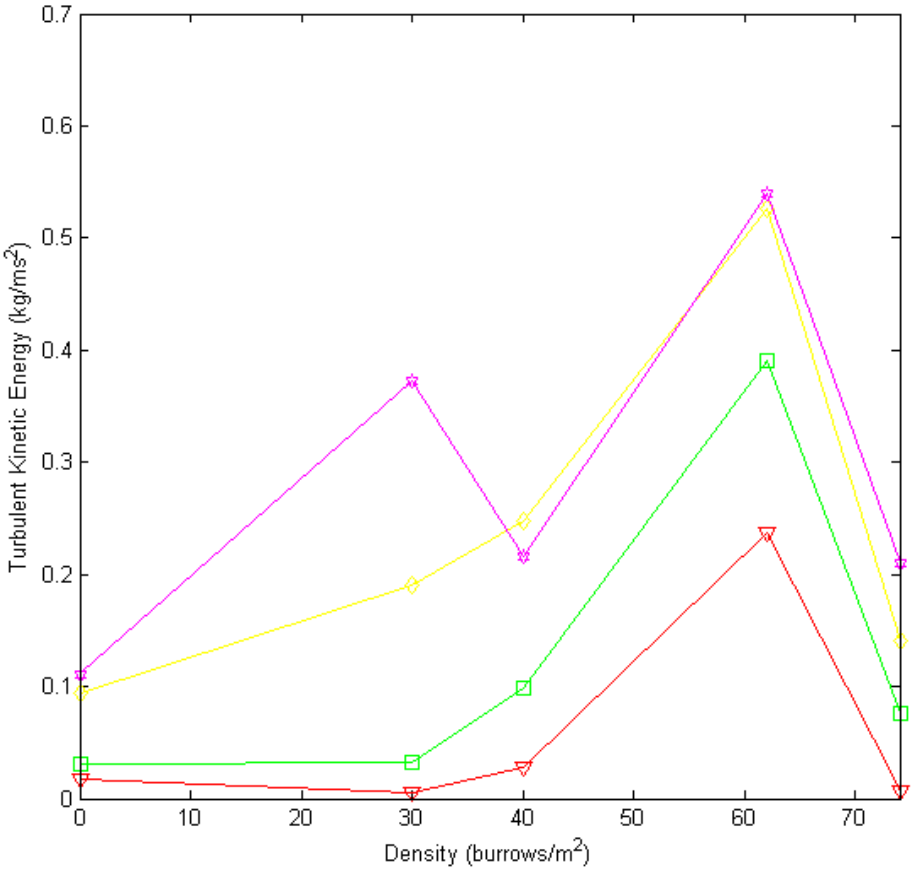

Figure 34: Burrow density (burrows/m^2) vs. mean turbulent kinetic energy at four flow speeds in the field. Both natural and artificial experimental data is shown. Colours/markers (red/triangles, green/squares, yellow/diamonds, and pink/stars) indicate nominal flow speeds of around 2, 5, 7, and 10 cm/s.

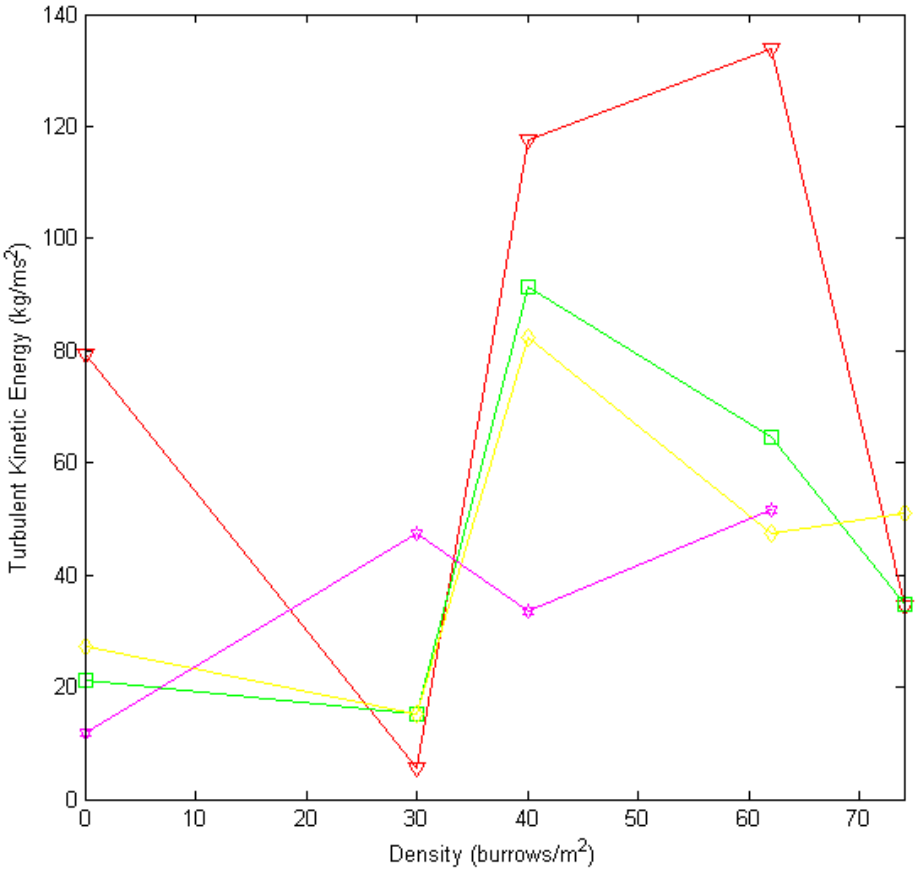

Figure 35: Normalised data of burrow density (burrows/m^2) vs. mean turbulent kinetic energy at four flow speeds in the field. Both natural and artificial experimental data is shown. . Colours/markers (red/triangles, green/squares, yellow/diamonds, and pink/stars) indicate 'nominal' flow speeds of 2, 5, 7, and 10 cm/s.

3.3.4 Sediment Trapping

Results from sediment trapping analysis (methodology section 2.2.3) showed that the dense burrow patch caught an average of 1.95 g/L of suspended sediment per burrow whereas the sparse burrow patch contained 1.66 g/L of suspended sediment per burrow (Figure 36). These values equated to 0.91 mg/cm^2 of sediment caught in the dense array compared with 0.42 mg/cm^2 caught in the sparse array, or 0.009 and 0.004 kg of sediment trapped per m^2, or 9.1 and 4.2 tonnes of sediment trapped per km^2, respectively.

In this experiment, the dense array caught more sediment, however the standard error $(standard\ deviation/\sqrt{n})$ between the two densities in Figure 20 was just large enough that there was overlap, so the average sediment caught in the two treatments may not be significantly different, and a standard t-test showed a non-significant p value of 0.3.

All the sediment caught within the artificial burrows had a combined smaller mean grain size than the surface sediment in the bed around the area. The trapped sediment had a much higher silt content when compared with the sediments sampled in the measurement areas (Table 4).

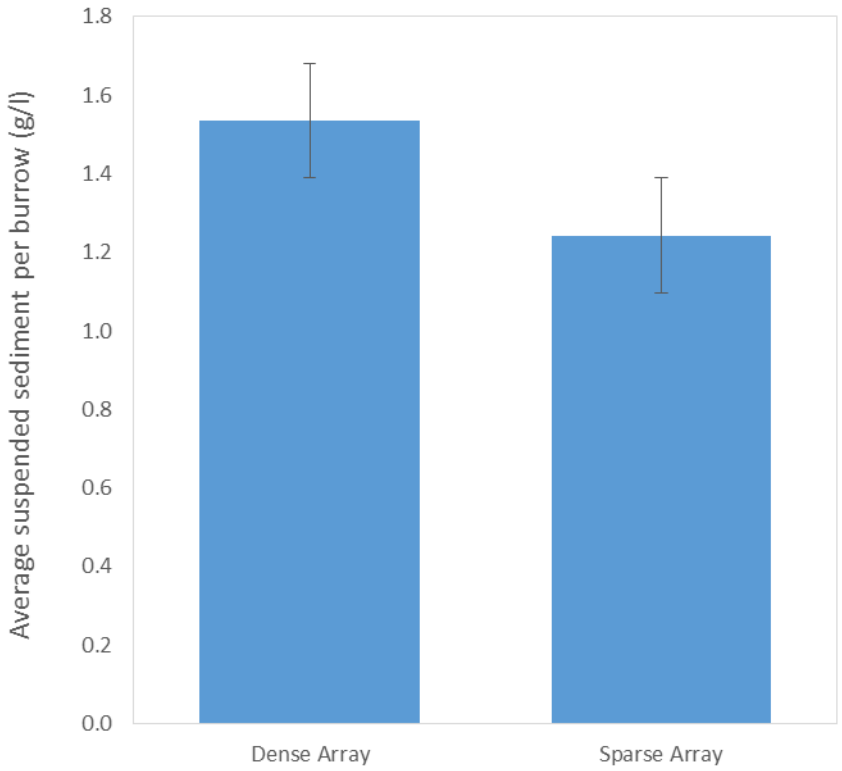

Figure 36: Average amount of suspended sediment caught within the burrow arrays buried in the field at Tairua.

Table 4: Summary of grain sizes found in the field sites and caught within the artificial burrows.

Site		Grain size (%)		
		Clay	Silt	Sand
Natural	Dense	0.17	15.90	83.83
	Sparse	0	9.91	89.77
	Control	0.03	9.65	89.97
Artificial	Dense	0	5.08	94.81
	Sparse	0	7.49	92.44
	Control	0	4.87	95.01
Caught in burrows		0.05	20.5	79.16

On average the burrows closest to the centre of the field arrays caught less than those situated on the outer edges (Figure 37, Figure 38). There was no discernible pattern in burrow orientation in the burrow arrays.

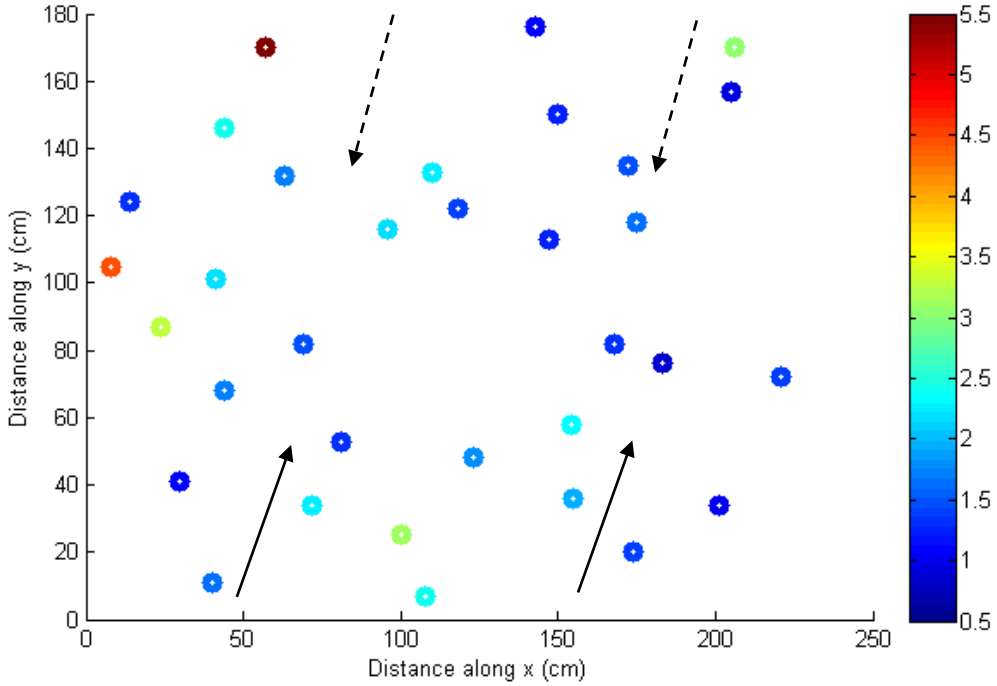

Figure 37: Spatial plot showing the amount of sediment caught (g suspended sediment caught/L) in each burrow for the dense array. Solid and dashed arrows indicate mean direction of incoming (flood) and outgoing (ebb) tidal flows, respectively.

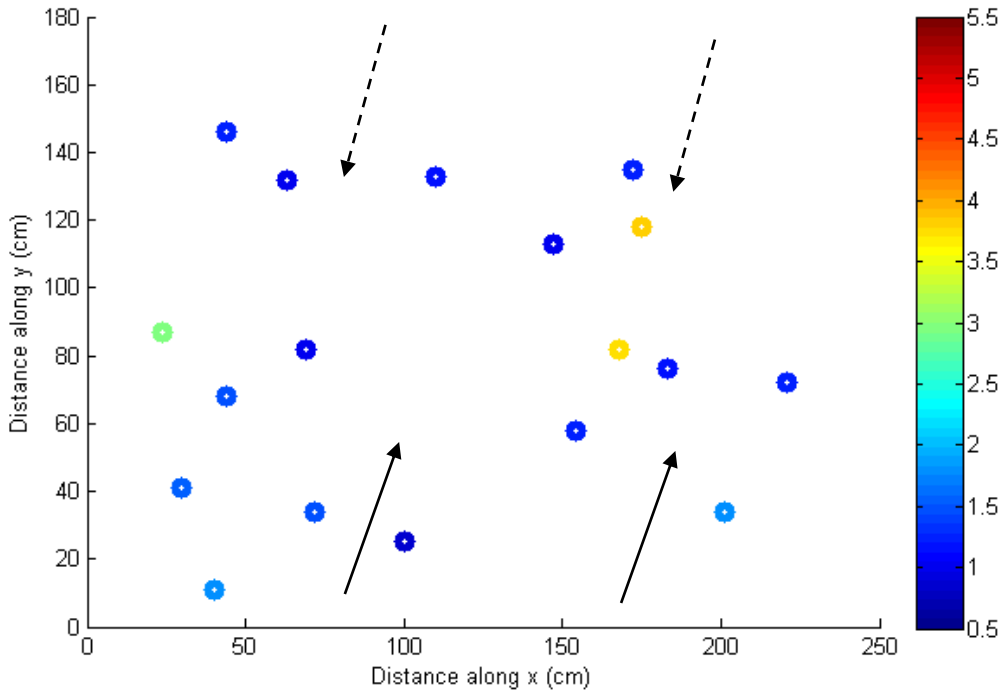

Figure 38: Spatial plot showing the amount of sediment caught (g suspended sediment caught/L) in each burrow for the sparse array. Solid and dashed arrows indicate mean direction of incoming (flood) and outgoing (ebb) tidal flows, respectively.

CHAPTER FOUR: DISCUSSION

4.1 Introduction

This study was the first to encompass fine resolution measurement of flows around crab burrows both in the laboratory and in the field. The primary objective was to elucidate the effects of *austrohelice crassa* burrows on near-bed flows and sediment trapping. A particular focus was placed on the effect of burrow density on flows; laboratory and field experiments were designed to fit this purpose. From these experiments, large amounts of data were collected which revealed differences in flow and sediment trapping between the various treatments tested. In particular, a link was found between turbulent kinetic energy (TKE) and burrow density in both the field and laboratory.

4.1.1 Individual Burrow

In the individual burrow experiments, a single burrow was used in various orientations to explore the effect of burrow orientation on flows and to quantify how water flows into and around a single burrow in a controlled laboratory environment. When no burrow was present, as expected, the near-bed flow in the flume exhibited a typical boundary layer profile. However, when a burrow was placed directly below the instrument, the flows were shown to be entering the burrow a small way, as may be expected based on previous findings in which modified boundary layer profiles were found to penetrate into topographic pits (Davies, 1982).

Although small, there was a noticeable difference in flow for different burrow orientations, with the most pronounced change being the depth to which the flow penetrated into the burrows. When the burrow was aligned with the flow, pointing directly downstream, the flow was able to penetrate slightly deeper into the burrow. It may be that when the burrow is oriented in-line with the flow that flow is more easily "pushed" into the burrow. This penetration did not show signs of being flow-speed dependent. Evidence of flow penetration into the burrow was shown by flow speeds greater than zero below the bed. However, acoustic reflections likely render precise measurements of velocities far into the burrow unreliable. Such reflections may explain the much deeper below-bed peaks (at depths of ~ -5 mm) in Figure 17. Flow extending into the burrows will create eddies near the bed, potentially affecting sediment movement (Figure 39).

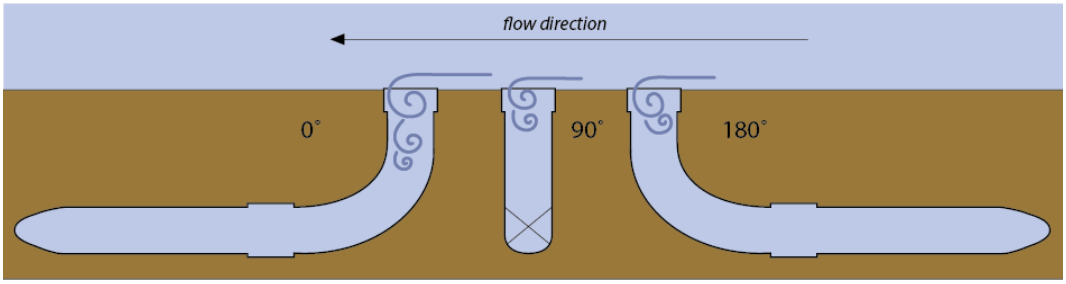

Figure 39: Schematic showing how eddy generation may occur within the burrows. The flow penetration appears to be affected by the burrows orientation to flow. Flows penetrate deeper into the burrow that is oriented with the closed end along the flow (0°, on the left), and less deeply into burrows with their closed ends oriented across (90°, middle) or into the flow (180°, right).

The profiles of flow upstream, downstream, and above the burrows in each orientation (Figure 19, Figure 20, and Figure 21) showed that consistently that the downstream profile reached further into the burrow when it was at 0° orientation. It

was to be expected that flows upstream of the burrow remained unaffected, while the downstream flows show the modification as a result of the flow encountering a change in bed drag resistance due to the presence of the burrow.

When the burrow array was constructed, the orientations of the burrows were varied as close to randomly as possible whilst achieving the highest burrows/m^2 possible. Given this consideration, the burrow array experiments should not be biased heavily by any of the aforementioned orientation affects. Since *austrohelice crassa* do not appear to orient their burrows in any particular manner (H. Needham, personal communication, 9 July, 2015), this approach was used to give a reasonable approximation of natural conditions.

4.1.2 Burrow Array

The results from this study indicate that burrow density has an influence on near-bed flows. When the burrow array was placed in the flume, as expected, turbulent kinetic energy (TKE) increased with flow speed, regardless of density. In profile, the TKE increased to the highest values just above the bed surface, similar to previous findings with emergent structures, where TKE is also greatest at the canopy-surface convergence (Lefebvre et al., 2010). The effect of increasing burrow density appeared flow speed dependent, with low flow speeds exhibiting a different response to increased burrow density to high flow speeds.

For low speeds that with higher burrow density, TKE appears to increase with burrow density up to a peak at approximately 20-40 burrows/m^2 and subsequently decreases. This peak may indicate a transition zone, where turbulence

is at a maximum for moderate burrow numbers, followed by a decline which may indicate a skimming flow regime.

A possible physical explanation for this decline in TKE with increasing burrow density may be obtained by considering the near bed drag force. Water flowing past the bed layer experiences greater drag at the bed surface when there are fewer burrows interspersed with small patches of water, where the burrows/holes are. The resistance between a water-on-sediment interface is larger than that exerted by a water-on-water interface. When there are more burrows/holes, there are more patches of water along the bed, reducing the overall drag force, and decreasing the turbulence. As burrow density increases, the proportion of water-on-water versus water-on-sediment interface increases. At these higher densities, the flow interacts less with the bed and acts more like a 'skimming flow' in which the burrows are seen more as an enhanced roughness than single obstructions. Skimming flow has been found in multiple studies of emergent structures, where increased structure density creates skimming flows which in turn leads to a reduction in sediment erosion from the bed (Widdows, Pope, Brinsley, et al., 2008; Nepf, 2012).

At the lower flow speeds, water is not flowing as quickly over the burrow entrances, potentially creating a greater opportunity for intrusion of flow into the burrows, and eddy generation. In these cases, there is enhanced water exchange, and more turbulence generated between the burrows and the above-bed area. However, as the burrow density increases, this effect becomes less significant than the reduction of drag with increased burrow density. The combination of the two effects at low flow speeds may explain the peak at 20-40 burrows/m^2.

For the high flow speeds, there was no apparent trend over most of the range of burrow densities tested. However, for the highest burrow density there was a sharp increase in TKE (Figure 25). This sharp increase also occurs at the lower, more intermediate flow speed of 5 cm/s. It may be that for higher flow speeds, the effect of increasing burrow density only becomes significant at higher burrow densities, beyond the range that was tested in this experiment. The speeds tested in this experiment were chosen to represent those commonly experienced on tidal flats where *austrohelice crassa* typically reside, as was shown in the field experiments.

4.1.3 Field Arrays

In the field it was observed that for artificial burrow arrays the TKE increased with increased burrow density to a peak at the sparse burrow array density (40 burrows/m^2), before decreasing again for the highest burrow density (74 burrows/m^2). This pattern is similar to findings from the laboratory burrow array experiments, with a potential transition in flow regime at approximately 40 burrows/m^2. Reasoning for this transition is likely to be similar to that outlined above (section 4.1.2).

For the natural crab burrows, the pattern for burrow density versus TKE which was found both in the laboratory and for the artificial crab burrows was not observed. It may be that the flow regime transition point exists beyond the range of densities tested or does not exist. Within the Pepe Inlet there were no patches of *austrohelice crassa* burrows exceeding the density of the 62 burrows/m^2 used, however burrow densities of up to 207 burrows/m^2 have been previously reported within the greater Tairua Harbour area (Needham et al., 2010). A future experiment

could examine if there is a transition to skimming flow that occurs within these denser patches of crab burrows in mud.

When both the artificial and natural results are combined (Figure 31), it becomes evident that at the higher flow speed (~10 cm/s) TKE is less affected by the influence of increasing burrow density. This difference in flow response between high and low flow speeds is similar to that found in the laboratory experiment where the high flow speeds also did not exhibit a strong response to increasing burrow density. As in the laboratory experiment, the 10 cm/s flow speed shows a sharp increase in TKE toward the highest burrow density tested.

4.1.4 Sediment Trapping

On average, the dense burrow array caught more sediment over the tidal cycle than the sparse burrow array. This finding was not deemed statistically significant by t-testing, however it may still be a real result, warranting more investigation. Such a difference in sediment trapping rates between dense and sparse patches would equate to a sediment trapping of 9 g of sediment trapped per m^2 in dense patches, compared with 4 g of sediment trapped per m^2 in sparse patches over a single tidal cycle. Over longer time periods this amount of trapping may become significant. Assuming New Zealand's tides are predominantly lunar semi-diurnal (M_2, occurring every 12.4 hours), there are on average 706 tidal cycles in a year, the dense patch would trap 6.42 $kg/m^2/yr$ of sediment, and the sparse 2.97 $kg/m^2/yr$. Volumes trapped of this magnitude have considerable potential to alter the morphology of tidal flats. It must however be noted that this rough value does not consider the excavation of sediment from the creation of burrows alongside this

trapping potential. Since the dense array caught more sediment, it can be cautiously concluded that there is a feedback between burrow density and sediment movement. This link may become more vital in sustaining the balance of sediments within tidal flats as sea level rise affects the environment into the future, and further work on quantifying the burrow-sediment interaction may be able to be incorporated into biomorphodynamics of numerical models (Coco et al., 2013).

The peak in TKE coincides with the sparse array (at 40 burrows/m^2), where it is likely that the higher turbulence kept the sediment in suspension, thus less sediment is caught within this array. However, as the burrow density increases to 74 burrows/m^2 in the dense array, skimming flow may develop, where TKE decreases, and more sediment can settle. In this respect, the higher sediment trapping and deposition that occurred in the dense array is as expected.

Bouma et al. (2007) found that sedimentation within dense patches of epibenthic structures was higher than in sparser patches. This finding suggests that increased sediment trapping with increased burrow density may have a similar feedback behaviour to emergent structures. The paper showed that the cause for the difference in sedimentation was likely due to shear stress differentials within the patches. Conversely, other work looking at epibenthic worm tubes has found that tubes of increasing density reduced erosion and deposition of suspended matter, but densities above 5% (area) showed a switch from net erosion to net deposition (Friedrichs et al., 2009).

It has been found that for increasing densities of *austrohelice crassa* burrows, there is a reduction of sediment eroded at reasonably high flow speeds in

sandy-mud, and a peak in erosion rates at middle densities for sandy sediment (Needham et al., 2013). The finding for sandy-mud corresponds well with the results in sediment trapping found in the present study, although the sediment in which the artificial arrays were buried was less muddy compared to the natural burrow arrays. Additionally, the densities measured in Needham et al. (2013) fell either below or significantly above the densities of the sparse and dense arrays, respectively.

The burrows trapped sediment which had a finer overall grain size and a higher proportion of fines than the surrounding sediment. Previously, Botto and Iribarne (2000) found that burrows that were permanently open captured organic matter rich clay and silt. Although only two arrays were used, if burrows capture a higher proportion of fines, if robust, this result may have significant implications for nutrient movement. Often organic matter has a smaller grain size, and so if more fines are caught in the burrows than exist in the surrounding surface area, then it is likely that the nutrient balance of the sediment will be affected by burrow density. Capture of reactive organic matter, and potential subsequent mineralisation may be occurring within the burrows, which is an important role in sustaining the recycling of nutrients (D'Andrea et al., 2002).

Generally, where the sediment is muddier, there are higher densities of crab burrows found (Morrisey et al., 1999; Needham et al., 2010). This appeared to be true for the sites measured within the Pepe Inlet for this study. Finding more crab burrows where the sediment is muddier may be indicative of a feedback between crab burrow building and sediment composition. Comparable feedbacks on tidal flats between vegetation and sediment movement have been discovered where

muddification occurred in dense assemblages of seagrass (van Katwijk et al., 2010). Since the crab burrows appeared to capture finer sediment than the surrounding surface area, it may be that over time, where crabs are present, the sediment becomes muddier, and more crabs colonise the area, making it even muddier faster.

The sediment trapped within the burrows occurred over an entire tidal cycle which precludes information on whether more sediment was caught during the flood, slack, or ebb tide, or if any was removed from the burrows. To determine the magnitudes of directional movement of sediment within the tidal flat, it would be useful to measure the sections of the tidal cycle separately, taking separate measurements for sediment trapped during the flood, slack, or ebb tide. There was visual indication of the flood and ebb flows carrying different sediment loads, with the incoming tide containing larger values of suspended sediments/particles during the very early stages of the tide (before the instruments were submerged, Figure 40), and tidal asymmetry within the inlet may influence the amount of sediment caught within each part of the tide. However, it has been found that a single tidal cycle may be insufficient in fully replacing burrow water (Hollins et al., 2009), and so nutrients and sediments may remain within the burrow over significant time periods.

Figure 40: Flood tidal waters inundating the artificial burrows control site.

Overall, there was no discernible effect of orientation on sediment trapping within the buried artificial arrays. However, a future study could examine in detail the effect of orientation on sediment trapping, given that there is a difference in penetration depth into the burrows between different orientations. To achieve this, it would be necessary to isolate the orientation effect from other variables by creating multiple burrow arrays containing burrows of a single orientation, with differing densities.

Lightly windy conditions dominated the tidal flat on the days of measurement, which is typical for the area. Although results featuring hydrodynamics focussed on times with minimal/no waves, the effect of waves cannot be excluded from the effects influencing the sediment results. It is possible that wind waves enhanced the amount of sediment within the water column available for trapping by the crab burrows. Wind waves have been shown to be a significant driver of sediment suspension and erosion in intertidal environments (Green & Coco, 2007; Widdows, Pope, & Brinsley, 2008), and so wind wave

generation may be a significant control on sediment trapping by burrows, and therefore this sediment trapping may vary seasonally. Moreover, previous research has found that where highly turbulent flow exists, sediment trapping by pits is diminished as bed shear increases (Yager et al., 1993). In this same paper, it was found that at low flow turbulence, such as occurred mostly at low flow speeds in the present study, the aspect ratio of the pits determined the sediment trapping, whereas at high turbulence, which often coincides with high flow speeds the turbulence determines the amount of deposition. Following these results, it may be concluded that during periods of high waviness, there would be little sediment capture. Exploration into differing burrow sizes and burrow entrance geometry would be useful to further elucidate the relative impact of wave-driven turbulence upon sediment trapping by burrows.

4.1.5 Limitations of Current Work

Although both the laboratory and field studies were designed to minimise the effects of confounding factors during experimentation, there were some discrepancies and unexpected occurrences which produce a few caveats on some of the findings reported.

The measurements for the laboratory burrow density analysis at the 15 cm/s speed were taken at a different time to the rest of the speed measurements. Differences between the 1, 2, 5, 7, 10 cm/s and the 15 cm/s (Figure 26) measurements suggest that there may perhaps have been inconsistencies in the running of the experiments or the flume ran differently when left to run at the same speed without change for an extended period of time. To resolve this question it

would be necessary to repeat a set of experiments which increment through the whole speed range.

The burrow array only represented one burrow shape/size. Even though the size and shape chosen for the burrows was taken from data indicating these dimensions as the most common, there was variation present in the natural burrow arrays that was not represented in the artificial burrow arrays. The burrow structure varies depending on both the activity, size, form, and feeding of the crab, and on varying environmental conditions including the sediment type (Kristensen & Kosta, 2005). A study by Yager et al. (1993) found that that when the aspect ratio of a pit is relatively wider, the concentration within the pit decreased. There is potential that the aperture of the artificial burrows may have had a significant effect on the amount sediment trapping that occurred. Natural burrows also have the potential to have multiple openings, which can be shown to induce complex flow behaviour and exhibit the potential for reasonably fast flushing periods (Ridd, 1996; Stieglitz et al., 2000; Heron & Ridd, 2001). Using burrows of only one shape, and with only one burrow opening allows for isolation of effects, but may only be partially representative of the overall effect of crab burrows on flow.

Figure 41: Dense natural field array site. The crab burrows present here were of varying sizes, and likely also varied in sub-surface shape.

Previous flume studies have been able to link observations made within the laboratory to field observations with reasonably few caveats (Bouma et al., 2007). A study by Bouma et al. (2007) attempted to link findings from a unidirectional flume (similar to that used in the present study) to a coupled field experiment exploring the effect of varying densities of emergent structures with sedimentation. They found that the flume study was unable to represent all scales that operate in estuarine functioning, and that flow artefacts affected the flume measurements. The same can be concluded for the present study where, by definition, the flume could not encompass all of the variables, scales, and three dimensionality that would affect real flows around crab burrows in the natural environment.

With the field arrays, there were only two densities measured so it is more difficult to pinpoint the transition zone where the flow regime may be switching. It would have been ideal to measure a wider range of arrays at the same time to capture the effects of a larger range of densities, however this was not possible due to lack of instrumentation.

The TKE showed an increase with increased burrow density, followed by a decrease in the artificial burrows, however for the natural burrow treatments, this pattern was not observed. A potential explanation for the difference in TKE response to increased burrow density may be that the artificial array does not behave exactly in the same way as the natural burrows. The artificial arrays were a human-made mimic which, by nature, cannot exactly represent the intricacies and variations existing in natural crab burrow arrays. While care was taken to ensure that the buried artificial burrows were flush with the surface of the sediment, it may be that the entrance geometry of the artificial burrows did not interact with the flow and surrounding sediment in precisely the same way as the natural crab burrows. Another potential discrepancy between the two burrow types may be the material that the artificial burrows were made of. The differences in porosity and roughness of the crab burrow walls between the artificial burrows and natural burrows may have influenced how flows respond to the crab burrows, although this is not likely to be a large effect. The environmental conditions on the two days were different, affecting the comparability of the data sets. The 9th was windier than the 10th of July, generating more waves. Unfortunately some of the field data was too wavy or of inadequate quality for analysis, with some speeds not being captured within the measurement times, and other data being deemed as too wavy for appropriate

analysis. This resulted in some gaps in the reported field data. The data that was used from the field experiments was trimmed manually to remove the parts with the most waves. During this process, it is possible that some of the data, particularly at the lowest flow speed (Figure 31), was still not completely devoid of waves. It has been found that surface waves can induce significant oscillatory motion within burrows (Webster, 1992), which may have occurred during this study, however as no measurements were taken immediately above burrows during the field experiments, it cannot be ascertained whether oscillatory movement penetrated into the burrows.

All of the sites chosen within the Pepe Inlet were of comparable grain size, being all classed as fine sand on the Wentworth Scale. The sites were set up carefully to minimise the influence of environmental differences affecting the flow in different ways between sites. All sites were of a similar orientation, and were set up so that the Vectrino Profiler frames were oriented so as to not affect the main incoming or outgoing flows over the burrow patches. Despite these considerations, it is possible that the measurements could have been affected by microscale or small changes in topography affecting flows.

More fine sediment appeared to be trapped by the burrows, however compared with the grab samples from the measurement sites (which had weeks of digestion), due to time constraints, the samples taken from the burrows did not undergo a very long period of organic digestion (hours) before being measured in the Laser Sizer, potentially leading to incomplete digestion and a small relative overrepresentation of fine material within the sediment caught in the burrows. This affect is however not likely to be large, as the majority of the digestion occurs

within the first two hours of sample preparation. This result of capturing fines within the holes is however consistent with findings in previous work (Yager et al., 1993; Botto & Iribarne, 2000). Previously, sediment traps similar to the artificial burrows used in this experiment have been deployed and have been found to be effective in measuring bedload sediment transport in shallow intertidal areas (Emerson, 1991). However, it was found that the traps may underestimate sediment transport due to skips from saltating material. The same effect may have affected the burrow sediment trapping, as the artificial burrow patches were limited in size.

Further study into how crab burrows affect near-bed flows could address some of the limitations encountered in carrying out the present study, and endeavour to minimise their effects.

4.2 Summary of Major Findings

The effects of crab burrows on near-bed flows were quantified both in a field, and a laboratory setting. An artificial burrow was created and fine resolution measurements of flows around single burrows in three different orientations were made in a unidirectional flume. The effects of burrow density on flows were measured in the flume, using multiple artificial crab burrows. These burrows were then taken into the field and measurements of these burrow arrays, and *in situ* natural burrows were made to find links in the effect of burrow density on flows between laboratory and field conditions.

The major findings of these experiments were:

1. The orientation of a single burrow affected flow penetration depth into the burrows. All orientations created a modified boundary layer, however the flow penetrated to the greatest depth when the burrow was oriented at 0° to the flow.
2. Increasing burrow density in the laboratory led to a split in flow regimes between high and low flow speeds. At low flow speeds, the TKE increases to a peak at approximately 20-40 burrows/m^2, before tapering off, as skimming flow likely develops. Overall, at high flow speeds there does not appear to be a relationship between TKE and burrow density, however there may be a response visible at the highest burrow density (74 burrows/m^2).
3. In the field experiments for the artificial burrow array, TKE appeared to increase to a peak at the sparse burrow density (40 burrows/m^2), and

decreased again at the dense burrow density (74 burrows/m^2). This relationship is similar to that found in the burrow array laboratory experiment, where skimming flow may be developing at high burrow densities.

4. For the natural burrow array, the TKE increased with burrow density. It is possible in this situation that skimming flow may develop beyond the range of tested burrow densities (0 - 62 burrows/m^2).
5. For all field experiments, when the results are combined a split in flow regimes between high and low flow speeds emerges. Similar to patterns observed in the laboratory experiments, the high flow speed did not exhibit the same peak in TKE at ~40 burrows/m^2, whereas the lower speeds showed evidence of the development of skimming flow with increased burrow density above ~40 burrows/m^2.
6. In the artificial crab burrows for the field experiments, the dense array trapped a greater amount of sediment (1.95 g/L) compared with the sparse array (1.66 g/L) (ns).
7. Overall, it appeared that the sediment caught within the burrows had a finer grain size, with a greater proportion of silt when compared with the surface sediment collected from the burrow measurement sites.

4.3 Future Work

Through burrow building of different densities, *austrohelice crassa* are proven ecosystem engineers, and so further research into the interactions between varying density assemblages of these burrows will likely elucidate the extent of alteration and influence on the environment that *austrohelice crassa* exert. In particular, the individual behaviour of these crabs may have significant influence upon the sediment movement, and also thus affect nutrient movement.

To enhance the scale of this study, the effects of higher densities of crab burrow could be added into the data sets to determine better the overall impact of increasing burrow density upon near-bed flows, and therefore potentially sediment movement. Measurements at higher burrow densities both in the laboratory and the field would be particularly useful at high flow speeds to determine whether skimming flow develops at higher densities for these flow speeds.

In the sediment trapping experiments conducted in the field, there was no discernible pattern with burrow orientation, however any relationship may have been obscured by other factors. To elucidate better the relationship between orientation and sediment trapping it would be necessary to isolate the burrow orientation from other variables. Sediment trapping could also be measured over partial tidal cycles to discern the major direction from which trapped sediment likely originates.

REFERENCES

Allanson, B. R., Skinner, D., & Imberger, J. (1992). Flow in prawn burrows. *Estuarine, Coastal and Shelf Science, 35*(3), 253-266. http://dx.doi.org/10.1016/S0272-7714(05)80047-2

Bell, R. G. (1994). Behaviour of dissolved silica, and estuarine/coastal mixing and exchange processes at Tairua Harbour, New Zealand. *New Zealand Journal of Marine and Freshwater Research, 28*(1), 55-68. http://dx.doi.org/10.1080/00288330.1994.9516596

Botto, F., & Iribarne, O. (2000). Contrasting Effects of Two Burrowing Crabs (*Chasmagnathus granulata and Uca uruguayensis*) on Sediment Composition and Transport in Estuarine Environments. *Estuarine, Coastal and Shelf Science, 51*(2), 141-151. http://dx.doi.org/10.1006/ecss.2000.0642

Bouma, T. J., van Duren, L. A., Temmerman, S., Claverie, T., Blanco-Garcia, A., Ysebaert, T., & Herman, P. M. J. (2007). Spatial flow and sedimentation patterns within patches of epibenthic structures: Combining field, flume and modelling experiments. *Continental Shelf Research, 27*, 1020-1045.

Chen, S. C., Chan, H. C., & Li, Y. H. (2012). Observations on flow and local scour around submerged flexible vegetation. *Advances in Water Resources, 43*, 28-37. http://dx.doi.org/10.1016/j.advwatres.2012.03.017

Coco, G., Zhou, Z., van Maanen, B., Olabarrieta, M., Tinoco, R., & Townend, I. (2013). Morphodynamics of tidal networks: Advances and challenges. *Marine Geology, 346*, 1-16.

D'Andrea, A. F., Aller, R. C., & Lopez, G. R. (2002). Organic matter flux and reactivity on a South Carolina sandflat: The impacts of porewater advection and macrobiological structures. *Limnology and Oceanography, 47*(4), 1056-1070.

Davies, A. G. (1982). The reflection of wave energy by undulations on the seabed. *Dynamics of Atmospheres and Oceans, 6*(4), 207-232. http://dx.doi.org/10.1016/0377-0265(82)90029-X

Day, P. (1965). Methods of soil analysis. In C. Black (Ed.), *Particle fractionation and particle-size analysis* (pp. 545-567). Madison, Winsconsin: American Society of Agronomy.

Emerson, W. C. (1991). A Method for the Measurement of Bedload Sediment Transport and Passive Faunal Transport on Intertidal Sandflats. *Estuaries, 14*(4), 361-371.

Franson, M. (1998). *Standard Methods for the Examination of Water and Wastewater* (20 ed.). Washington DC.

Friedrichs, M., Leipe, T., Peine, F., & Graf, G. (2009). Impact of macrozoobenthic structures on near-bed sediment fluxes. *Journal of Marine Systems, 75*(3-4), 336-347. http://dx.doi.org/10.1016/j.jmarsys.2006.12.006

Gibbs, M., Thrush, S., & Ellis, J. (2001). Terrigenous clay deposition on estuarine sandflats: Using stable isotopes to determine the role of the mud crab, *Helice crassa* Dana, in the recovery process. *Isotopes in Environmental and Health Studies, 37*(2), 113-131. http://dx.doi.org/10.1080/10256010108033288

Gilbert, F., Aller, R. C., & Hulth, S. (2003). The influence of macrofaunal burrow spacing and diffusive scaling on sedimentary nitrification and denitrification: An experimental simulation and model approach. *Journal of Marine Research, 61*(1), 101-125. http://dx.doi.org/10.1357/002224003321586426

Gilbert, F., Stora, G., & Bonin, P. (1998). Influence of bioturbation on denitrification activity in Mediterranean coastal sediments: an in situ experimental approach. *Marine Ecology Progress Series, 163*, 99-107. http://dx.doi.org/10.3354/meps163099

Green, M. O., & Coco, G. (2007). Sediment transport on an estuarine intertidal flat: Measurements and conceptual model of waves, rainfall and exchanges with a tidal creek. *Estuarine, Coastal and Shelf Science, 72*(4), 553-569.

Hawkins, A. J. S., & Jones, M. B. (1982). Gill area and ventilation in two mud crabs, *Helice crassa* Dana (Grapsidae) and *Macrophthalmus hirtipes* (Jacquinot) (Ocypodidae), in relation to habitat. *Journal of Experimental Marine Biology and Ecology, 60*(2–3), 103-118. http://dx.doi.org/10.1016/0022-0981(82)90153-8

Heron, S. F., & Ridd, P. (2001). The Use of Computational Fluid Dynamics in Predicting the Tidal Flushing of Animal Burrows. *Estuarine, Coastal and Shelf Science, 52*, 411-421.

Heron, S. F., & Ridd, P. (2003). The effect of water density variations on the tidal flushing of animal burrows. *Estuarine, Coastal and Shelf Science, 58*, 137-145.

Heron, S. F., & Ridd, P. (2008). The tidal flushing of multiple-loop animal burrows. *Estuarine, Coastal and Shelf Science, 78*, 135-144.

Hollins, S. E., Heron, S. F., & Ridd, P. (2009). Methods for monitoring tidal flushing in large animal burrows in tropical mangrove swamps. *Estuarine, Coastal and Shelf Science, 82*, 615-620.

Hume, T. M., & Herdendorf, C. E. (1992). Factors Controlling Tidal Inlet Characteristics on Low Drift Coasts. *Journal of Coastal Research, 8*(2), 355-375. http://dx.doi.org/10.2307/4297982

Kinoshita, K., Wada, M., Kogure, K., & Furota, T. (2003). Mud shrimp burrows as dynamic traps and processors of tidal-flat materials. *Marine Ecology Progress Series, 247*, 150-164.

Kristensen E, Kostka J. (2005). Macrofaunal burrows and irrigation in marine sediment; microbiological and biogeochemical interactions. In Kristensen E, Haese, R. R., Kostka., J.E. (Eds.), *Interactions Between Macro- and Microorganisms in Marine Sediments* (pp. 125-158) American Geophysical Union, Washington, DC

Laverock, B., Gilbert, J. A., Tait, K., Osborn, A. M., & Widdicombe, S. (2011). Bioturbation: impact on the marine nitrogen cycle. *Biochemical Society Transactions, 39*, 315-320. http://dx.doi.org/10.1042/bst0390315

Lefebvre, A., Thompson, C. E. L., & Amos, C. L. (2010). Influence of *Zosteramarina* canopies on unidirectional flow, hydraulic roughness and sediment movement. *Continental Shelf Research, 30*, 1783-1794.

Lhermitte, R., & Serafin, R. (1984). Pulse-to-pulse coherent Doppler sonar signal processing techniques. *Journal of Atmospheric and Oceanic Technology, 1*, 293-308.

Liu, Z. (2014). *Hydrodynamic and sediment transport numerical modelling and applications at Tairua Estuary, New Zealand.* (Doctoral thesis, University of Waikato, Hamilton, New Zealand).

Lohrmann, A., Hackett, B., & Røed, L. (1990). High resolution measurements of turbulence, velocity and stress using a pulse-to-pulse coherent sonar. *Journal of Atmospheric and Oceanic Technology, 7*, 19-37.

Lohrmann, A., & Nylund, S. (2008). *Pure coherent Doppler systems – how far can we push it?* Paper presented at the Current Measurement Technology 2008 Conference, Charlston.

López, F., & García, M. (1998). Open-channel flow through simulated vegetation: Suspended sediment transport modeling. *Water Resources Research, 34*(9), 2341-2352. http://dx.doi.org/10.1029/98WR01922

Miller, D. C., Norkko, A., & Pilditch, C. A. (2002). Influence of diet on dispersal of horse mussel *Atrina zelandica* biodeposits. *Marine Ecology Progress Series, 242*, 153-167.

Morrisey, D. J., DeWitt, T. H., Roper, D. S., & Williamson, R. B. (1999). Variation in the depth and morphology of burrows of the mud crab *Helice crassa* among different types of intertidal sediment in New Zealand. *Marine Ecology Progress Series, 182*, 231-242. http://dx.doi.org/10.3354/meps182231

Murray, J. M. H., Meadows, A., & Meadows, P. S. (2002). Biogeomorphological implications of microscale interactions between sediment geotechnics and marine benthos: a review. *Geomorphology, 47*(1), 15-30. http://dx.doi.org/10.1016/s0169-555x(02)00138-1

Needham, H. (2011). *The context-specific roles of a bioturbating crab (Austrohelice crassa) on ecosystem functioning.* (Doctoral thesis, University of Waikato, Hamilton, New Zealand).

Needham, H., Pilditch, C., Lohrer, A., & Thrush, S. (2011). Context-Specific Bioturbation Mediates Changes to Ecosystem Functioning. *Ecosystems, 14*(7), 1096-1109. http://dx.doi.org/10.1007/s10021-011-9468-0

Needham, H., Pilditch, C. A., Lohrer, A. M., & Thrush, S. F. (2013). Density and habitat dependent effects of crab burrows on sediment erodibility. *Journal of Sea Research, 76*(0), 94-104. http://dx.doi.org/10.1016/j.seares.2012.12.004

Needham, H. R., Pilditch, C. A., Lohrer, A. M., & Thrush, S. F. (2010). Habitat dependence in the functional traits of *Austrohelice crassa*, a key bioturbating species. *Marine Ecology Progress Series, 414*, 179-193.

Nepf, H. M. (2012). Flow and Transport in Regions with Aquatic Vegetation. *Annual Review of Fluid Mechanics, 44*(1), 123-142. http://dx.doi.org/10.1146/annurev-fluid-120710-101048

Nye, P. A. (1977). Reproduction, Growth and Distribution of the Grapsid Crab *Helice crassa* (Dana, 1851) in the Southern Part of New Zealand. *Crustaceana, 33*(1), 75-89. http://dx.doi.org/10.2307/20103193

Pritchard, D. W. (1967). What is an Estuary: Physical Viewpoint. In G. H. Lauff (Ed.), *Estuaries* (Vol. 83, pp. 757). Washington, DC: American Association for the Advancement of Science.

Ridd, P. (1996). Flow Through Animal Burrows in Mangrove Creeks. *Estuarine, Coastal and Shelf Science, 43*, 617-625.

Rusello, P. J. (2009). A practical primer for pulse coherent instruments. *Nortek Technical Note, 27*, 1-12.

Smith, T. J., Boto, K. G., Frusher, S. D., & Giddins, R. L. (1991). Keystone species and mangrove forest dynamics: the influence of burrowing by crabs on soil nutrient status and forest productivity. *Estuarine, Coastal and Shelf Science, 33*(5), 419-432. http://dx.doi.org/10.1016/0272-7714(91)90081-L

Snelgrove, P. V. R. (1999). Getting to the bottom of marine biodiversity: Sedimentary habitats - Ocean bottoms are the most widespread habitat on Earth and support high biodiversity and key ecosystem services. *Bioscience, 49*(2), 129-138. http://dx.doi.org/10.2307/1313538

Stieglitz, T., Ridd, P., & Muller, P. (2000). Passive irrigation and functional morphology of crustacean burrows in a tropical mangrove swamp. *Hydrobiologia, 421*, 69-76. http://dx.doi.org/10.1023/a:1003925502665

Tang, M., & Kristensen, E. (2007). Impact of microphytobenthos and macroinfauna on temporal variation of benthic metabolism in shallow coastal sediments. *Journal of Experimental Marine Biology and Ecology, 349*(1), 99-112. http://dx.doi.org/10.1016/j.jembe.2007.05.011

Thrush, S. F., Hewitt, J. E., Norkko, A., Cummings, V. J., & Funnell, G. A. (2003). Macrobenthic recovery processes following catastrophic sedimentation on estuarine sandflats. *Ecological Applications, 13*(5), 1433-1455. http://dx.doi.org/10.1890/02-5198

van Katwijk, M., Bos, A., Hermus, D., & Suykerbuyk, W. (2010). Sediment modification by seagrass beds: Muddification and sandification induced by plant cover and environmental conditions. *Estuarine, Coastal and Shelf Science, 89*, 175-181.

Warren, J. H., & Underwood, A. J. (1986). Effects of burrowing crabs on the topography of mangrove swamps in New South Wales. *Journal of Experimental Marine Biology and Ecology, 102*(2–3), 223-235. http://dx.doi.org/10.1016/0022-0981(86)90178-4

Webb, A. P., & Eyre, B. D. (2004a). Effect of natural populations of burrowing thalassinidean shrimp on sediment irrigation, benthic metabolism, nutrient fluxes and denitrification. *Marine Ecology Progress Series, 268*, 205-220. doi: 10.3354/meps268205

Webb, A. P., & Eyre, B. D. (2004b). The effect of natural populations of the burrowing and grazing soldier crab (*Mictyris longicarpus*) on sediment irrigation, benthic metabolism and nitrogen fluxes. *Journal of Experimental Marine Biology and Ecology, 309*(1), 1-19. http://dx.doi.org/10.1016/j.jembe.2004.05.003

Webb, A. P., & Eyre, B. D. (2004c). The effects of two benthic chamber stirring systems on the diffusive boundary layer, oxygen flux, and passive flow through model macrofauna burrows. *Estuaries, 27*(2), 352-361. http://dx.doi.org/10.1007/bf02803391

Webster, I. T. (1992). Wave enhancement of solute exchange within empty burrows. *Limnology and Oceanography, 37*(3), 630-643.

Widdows, J., & Brinsley, M. (2002). Impact of biotic and abiotic processes on sediment dynamics and the consequences to the structure and functioning of the intertidal zone. *Journal of Sea Research, 48*(2), 143-156. http://dx.doi.org/10.1016/S1385-1101(02)00148-X

Widdows, J., Pope, N., & Brinsley, M. (2008). Effect of *Spartina anglica* stems on near-bed hydrodynamics, sediment erodability and morphological changes on an intertidal mudflat. *Marine Ecology Progress Series, 362*, 45-57.

Widdows, J., Pope, N., Brinsley, M., Asmus, H., & Asmus, R. (2008). Effects of seagrass beds (*Zostera noltii* and *Z. marina*) on near-bed hydrodynamics and sediment resuspension. *Marine Ecology Progress Series, 358*, 125-136.

Xin, P., Jin, G., Li, L., & Barry, D. (2009). Effects of crab burrows on pore water flows in salt marshes. *Advances in Water Resources, 32*, 439-449.

Yager, P. L., Nowell, A. R. M., & Jumars, P. A. (1993). Enhanced deposition to pits: A local food source for benthos. *Journal of Marine Research, 51*(1), 209-236. http://dx.doi.org/10.1357/0022240933223819

Ziebis, W., Forster, S., Huettel, M., & Jorgensen, B. (1996). Complex burrows of the mud shrimp *Callianassa truncata* and their geochemical impact in the sea bed. *Nature, 382*, 619-622.